MASTERTHESIS BIOMEDICAL ENGINEERING

CHARACTERIZING PROSTATE CANCER CELL LINES OF VARIED AGGRESSIVENESS AND EVALUATING THEIR RESPONSE TO ENZALUTAMIDE

YVETTE PETERS

06/07/2022

Department
Medical Cell Biophysics Group (MCBP)
University of Twente

Supervisors
Prof. Dr. L.W.M.M. Terstappen,
Dr. Ruchi Bansal
MSc E. Dathatri

External evaluator
Dr. H.J.G. Snippert
University Medical Center Utrecht

UNIVERSITY OF TWENTE.

Acknowledgement

I would like to thank Leon Terstappen and Ruchi Bansal for giving me the opportunity to carry out my master thesis at Medical Cell BioPhysics (MCBP) and for their expert advice and critical view throughout this project.

In addition, I would like to express my gratitude to my daily supervisor, Eswhari Dathathri, who guided me throughout this project. She was always able to meet and discuss all my questions.

I wish to acknowledge the help provided by the technical staff Christian Breukers, Anouk Mentink and Yvonne Kraan, and the other members of the MCBP group for their help with the experiments.

I would like to thank Hugo Snippert and Ingrid Verlaan for allowing me and Eshwari to follow a training to culture organoids, at the University Medical Centrum Utrecht.

Special thanks to my friends, family and boyfriend for their support during my master thesis.

Lastly, I would like to thank Leon Terstappen, Ruchi Bansal, Hugo Snippert and Eshwari Dathathri for their willingness to be part of the exam committee.

Abstract

Prostate cancer (PCa) is the most diagnosed cancer in men and it is the second leading cause of cancer-related death in Western societies. Despite improved treatments for metastatic prostate cancer patients, not all patients respond similarly thereby affecting overall survival. To reduce the frequent administration and ineffectiveness of treatments, there is a need for prognostic markers which can help predict the response of patients to therapies, making treatments more targeted and personalized.

In this study, we aimed to develop a realistic model to study the phenotypic response of PCa cell lines, towards androgen stimulation and inhibition. We performed a proteomic analysis (PSA secretion) of multiple PCa cell lines (LNCaP, PC-3, 22Rv1, RWPE-1, RWPE-2 and PWR-1E, EMC-PCa-41 organoid cells) derived from different stages of PCa, in response to androgen stimulation (R1881) and inhibition (Enzalutamide). We detected PSA secretion from different malignant PCa cell lines (LNCaP, 22Rv1, EMC-PCa-41) and observed absence of PSA secretion in the benign cell lines. This is confirmed with ELISA. In addition, PSA secretion from single LNCaP cells was identified and we observed that the PSA secretion of LNCaP cells is affected by the anti-androgen Enzalutamide. These results suggest that LNCaP cells can be used as a model mimicking the responses to anti-androgens in mHSPC patients.

However, this method fails to distinguish between PSA secretion from low-producing cell lines and artifacts. To overcome this, a microwell chip is recommended and more optimization on the quantification method must be done.

The PCa cell lines (LNCaP, PC-3, 22Rv1, RWPE-1, RWPE-2 and PWR-1E) were also phenotypically characterized using immunofluorescence staining (PSA, PSMA) and flow cytometry (PSMA, EpCAM, HER2). Our findings indicate PSMA, EpCAM, and HER2 expression in malignant PCa cell lines and the absence of PSMA expression in the benign cell lines. In addition, the hormone-sensitive LNCaP cell line shows higher levels of PSMA and HER2 expression compared to the benign and the castration-resistant cell lines.

Proteomic analysis of single cells can help identify prognostic biomarkers and develop an effective and personalised therapy for PCa patients. Using a PVDF membrane, LNCaP cells can serve as a good model to study the PSA secretion in response to drugs. In the future, a microwell chip can help to identify the effect of drugs and stimulation on PSA secretion from the other PCa cell lines.

Table of Contents

1. Introduction

1.1 Prevalence and diagnosis of prostate cancer

Prostate cancer (PCa) is the most diagnosed cancer in men and it is the second leading cause of cancer-related death in Western societies (Siegel, Miller, & Jemal, 2020). In the Netherlands alone, more than 12.000 men are diagnosed each year with PCa (IKNL, 2021).
In order to detect PCa, common screening procedures, like Digital Rectal Examination (DRE) or blood Prostate Specific Antigen (PSA) test are used. By performing DRE the doctor can feel abnormalities of the prostate. This does not confirm the presence of PCa and is therefore mostly used as an additional test to the PSA test. This PSA test is a non-invasive test in which blood is drawn to check PSA levels. Elevated PSA levels (≥ 4 ng/mL) could indicate PCa (Tikkinen et al., 2018)(Catalona, 2018). However, the elevated PSA levels could also be caused by other factors such as the age of the men or prostate inflammation (Tikkinen et al., 2018). To determine the reason for the elevated PSA levels, men can undergo an MRI scan and biopsy. By performing an MRI scan abnormalities around the prostate can be detected. Furthermore, an MRI scan can determine whether cancer has spread to other places in the body. With a biopsy, a small sample of tissue is taken from the prostate. This tissue sample is examined by histology and the biopsy results determine the aggressiveness of the tumor (Tikkinen et al., 2018)(Duffy, 2020). To monitor the tumor regression after treatment, blood PSA levels are evaluated and MRI scans are taken.

Of the diagnosed PCa patients, around 70% have localized prostate cancer (IKNL, 2021). The overall survival (OS) for patients with localised prostate cancer is very high, the relative 5-year survival rate is almost 100% (The American Cancer Society, 2020)(IKNL, 2021)(Ng, Smith, & Shamash, 2020). Therapies such as surgery or radiotherapy are in most cases successful in removing the localized tumor for these PCa patients.

1.2 PCa progression and metastasis

Despite receiving these treatments, some PCa patients experience biochemical recurrence (with increased PSA levels), without metastasis in distant regions leading to non-metastatic Hormone-Sensitive Prostate cancer (nmHSPC) (Figure 1, (Dathathri et al., 2022)). Patients can be

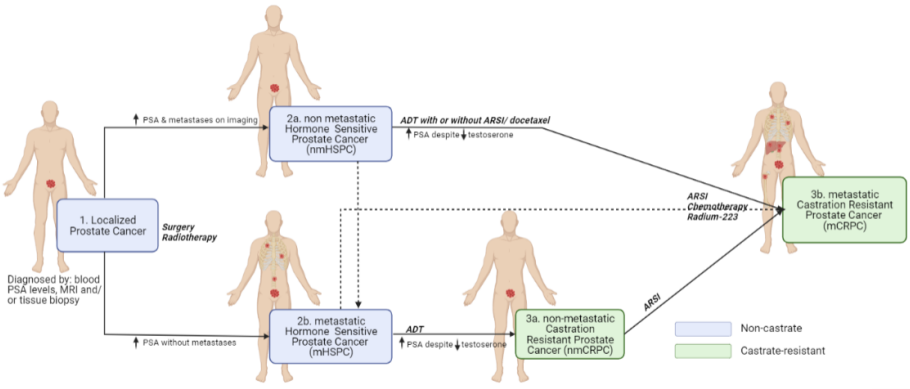

Figure 1: Disease states of PCa. PCa begins with localized PCa. This tumor is in most cases successfully removed using radiation or surgery. However, some patients are diagnosed again with increased PSA levels, this is referred to as (m)HSPC. The main therapy is ADT. However, overtime (m)HSPC patients can develop resistance to ADT. This is referred to as (m)CRPC. There is no curative treatment for this stage. However, to reduce cancer progression and symptoms mCRPC is treated with a combination of ARSi, Radium-223 and chemotherapy. (Dathathri et al., 2022)

diagnosed with metastasis in distant regions of the body, mainly bone, lymph nodes, liver and lungs, leading to metastatic Hormone-Sensitive Prostate Cancer (mHSPC). In both nmHSPC and mHSPC patients, the main therapy administered is androgen deprivation therapy (ADT), which helps to reduce androgen levels and thus inhibits tumor growth (Perlmutter & Lepor, 2007). ADT can be combined with androgen receptor signalling inhibitors (ARSi) and/or chemotherapy to treat mHSPC patients. However, over time, (m)HSPC can develop resistance to ADT and lead to (metastatic) Castration-Resistant Prostate Cancer ((m)CRPC), which is the end stage of the disease. Around 10-20% of the patients progress to this advanced disease stage (Vellky & Ricke, 2020)(Wade & Kyprianou, 2018). A curative treatment does not exist. However, to slow down the cancer progression, prolong survival and reduce symptoms, mCRPC is commonly treated with a combination of hormone therapy (ARSi), radiotherapy (radium-223) and chemotherapy (e.g. docetaxel) (Ng et al., 2020)(Wade & Kyprianou, 2018).

Despite the emergence of novel treatments for mHSPC and MCRPC, some patients do not respond to therapy and show poor OS, thereby rendering the treatment ineffective. There is a need for biomarkers to help in identifying, stratifying and monitoring patients who show poor OS, and to predict treatment. PSA is the most widely used biomarker for PCa. Biomarkers also provide the advantage of being less invasive compared to a tissue biopsy or MRI scan. In the next chapter, various potential biomarkers which can improve prognosis and help in developing personalized treatment will be discussed.

1.3 Biomarkers

Biomarkers are indicators of a medical state which can be measured accurately (Strimbu & Tavel, 2010). There exist a broad scale of different biomarker types. A few examples are blood biomarkers, lipids, extracellular vesicles (EVs) with their constituents, or circular tumor cells (CTCs). Overexpression or lack of certain biomarkers could have a diagnostic, predictive or prognostic value. In this chapter, PSA, PSMA, EpCAM and HER2 are discussed. PSA is a blood biomarker, a protein which is secreted by cells. PSMA, EpCAM and HER2 are all glycoproteins on the cell membrane.

1.3.1 Prostate Specific Antigen

PSA is a protein which is secreted by healthy as well as cancerous epithelial cells of the prostate gland and encoded by the KLK3 gene. PSA is present in the semen and blood of men with healthy prostates and is often elevated in men with prostate cancer, other prostate diseases or inflammation (Tikkinen et al., 2018).
PSA is the current gold-standard biomarker for screening, diagnosis and prognosis of PCa (Tonry, Finn, Armstrong, & Pennington, 2020). Testing the PSA levels in the blood of men is non-invasive and men with PSA levels ≥ 4 ng/mL are recommended for biopsy or MRI scan to find out whether the elevated levels are caused by PCa (Tikkinen et al., 2018)(Catalona, 2018).

However, there are some limitations to using PSA as a biomarker for PCa as well. Using PSA as a screening biomarker contributes to over-treatment. For only 33% of the men with raised PSA levels, a diagnosis with PCa is given. For this, an additional biopsy or performing an MRI scan is necessary (Tikkinen et al., 2018)(Catalona, 2018). This indicates that there are many men with elevated PSA levels who do not have PCa (false positive)(Tikkinen et al., 2018). Screening for elevated PSA levels can also lead to the detection of many low-risk tumors, many of which cases never cause significant harm to a patient and do not require treatment (Tonry et al., 2020). Furthermore, with PSA as a screening strategy for PCa, not all PCa cases will be found and false

negatives can be missed. Despite low PSA levels (≤ 4 ng/mL), around 15-20% of the men with low PSA levels have an aggressive form of PCa (Tikkinen et al., 2018)(Carm et al., 2019). These patients will not show up on the PSA blood level test.
Another limitation of PSA is that it is not able to differentiate between localized and aggressive metastatic forms of cancer and identify the heterogeneity in patient prognosis (Duffy, 2020)(Terada et al., 2017).
Despite these limitations, PSA remains the best validated and most prognostic biomarker for OS in metastatic Prostate Cancer (mPCa). C. Harshman et al. concluded that a PSA level ≤ 0.2 ng/mL at 7 months is prognostic for longer OS of mHSPC patients on ADT (Harshman et al., 2018). This seems promising. In the future, PSA should be combined with other biomarkers for determining tumour aggressiveness and predicting outcomes (Duffy, 2020).

1.3.2 Prostate-Specific Membrane Antigen

Prostate-Specific Membrane Antigen (PSMA) is a membrane protein and is expressed in all types of prostate tissue and often increased in prostate tumor cells and tumor tissue (Chang, 2004)(Chang, Reuter, Heston, & Gaudin, 2001). A new imaging technique is being explored for early detection of PCa metastasis or biochemical recurrence, called PSMA positron emission tomography (PET) (Donswijk et al., 2020)(Tsechelidis & Vrachimis, 2022). 68Ga-PSMA-11 is a radioactive imaging agent which binds to PSMA when it is injected into the patient. Due to overexpression of PSMA on cancerous tissues, PCa cells are localized and can be imaged using PET, which helps to indicate metastasis (Tsechelidis & Vrachimis, 2022). However, one of the limitations of this technique is that PSMA is not expressed in all prostate tumors. Additionally, PCa shows intra- and interpatient heterogeneity of PSMA expression (22). Further studies are needed to evaluate the diagnostic and therapeutic value of PSMA as a PCa biomarker.

1.3.3 Epithelial cell adhesion molecule

Epithelial cell adhesion molecule (EpCAM) is a transmembrane glycoprotein, which is commonly used to capture circulating tumor cells (CTCs) in the blood of cancer patients (Keller, Werner, & Pantel, 2019). In multiple carcinomas, including prostate cancer tissue, EpCAM is often overexpressed (Massoner et al., 2014)(Keller et al., 2019)(Ni et al., 2012a)(Ni et al., 2012b)(Liao, Wu, Jia, Mou, & Li, 2022). Research is done into EpCAM as a potential prognostic biomarker. Y. Liao et all discovered a close association between high EpCAM expression and poor PCa prognosis (Liao et al., 2022). In addition, due to overexpression of EpCAM in PCa, it is a promising target for PCa treatments. This is the most optimal in combination with targeting other pathways, based on individual tumor profiles (Ni et al., 2012b). More data is required to establish EpCAM as a prognostic biomarker or a potential EpCAM targeted therapy for PCa.

Met opmerkingen [PY(SMB1]: Mention the cell search system which employs epcam based enrichment to improve detection of CTCs.

1.3.4 Human epidermal growth factor receptor 2

Human epidermal growth factor receptor 2 (HER2) is an important prognostic biomarker in breast cancer. Breast cancer patients with overexpression of HER2 are called asHER2-positive. These patients can be treated with HER2-targeted therapies (Dent, Oyan, Honig, Mano, & Howell, 2013)(LI & LI, 2013). HER2 also drives the progression of other cancer types. However, the role of HER2 in the progression of PCa is poorly understood. Previous studies show contradicted results when studying the expression of HER2 in PCa. Immunohistochemical (IHC) analysis reported HER2 expression rates ranging from 0% to 100% (Day et al., 2017)(Sharifi et al., 2016). However, K.C. Day et al., and N. Sharifi et al., discovered both increased HER2 protein levels in PCa patients (Day et al., 2017)(Sharifi et al., 2016). Further studies are needed to evaluate the potential of HER2 as a PCa biomarker.

1.4 Therapies

As described previously, each stage of PCa is treated with different therapies. Localized PCa is usually treated with surgery or radiotherapy. In most cases this is very successful, the relative survival rate is almost 100%. This is in contrast to patients with mPCa. The OS rate for mPCa is around 30% (The American Cancer Society, 2020)(Dathathri et al., 2022). An improved outcome for these patients is crucial. mHSPC is usually treated with ADT and increasingly ADT is combined with ARSI or chemotherapy, as explained in this chapter.

1.4.1 Role of androgens in PCa

Prostate cancer is driven by androgens. Androgens are steroid hormones, such as testosterone. Testosterone is enzymatically converted into dihydrotestosterone (DHT) when it enters a cell, see Figure 2. DHT binds to the androgen receptor (AR) which results in dimerization and nuclear translocation of the AR. This is followed by binding to specific DNA sequences, androgen response elements (ARE), which increases the transcriptional activity of androgen-regulated genes, such as PSA, and promotion of prostate epithelial proliferation (Wade & Kyprianou, 2018)(Girling, Whitaker, Mills, & Neal, 2007). PCa progression is regulated by androgens through this pathway. Therefore, many therapies are based on targeting the AR. In 1941, Dr Huggins et al. demonstrated for the first time a relationship between androgen depletion and a reduction in clinical symptoms (Huggins, 1942)(Narayanan, 2020).

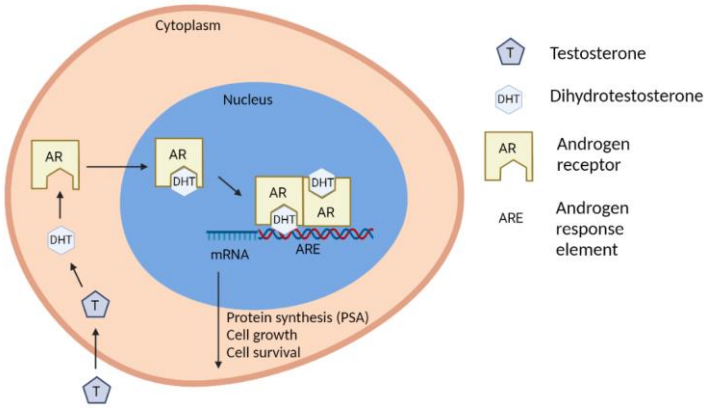

Figure 2: Schematic overview of the pathway of the androgen receptor (AR). Testosterone enters a cell and is converted into dihydrotestosterone (DHT). DHT binds to the AR and the AR translocates to the nucleus. This results in transcriptional activity, with cell growth, cell survival and protein synthesis as consequence.

Initially, the reduction of androgen levels causes tumor regression. However, when PSA levels increase despite low testosterone levels, PCa is classified as CRPC. The AR remains the driver in CRPC. However, the AR can adapt itself to the new environment so it does not require high androgen levels. Mechanisms are for example AR overexpression, in which the AR becomes hypersensitive to low levels of androgens. Or an AR mutation, which results in higher AR activity by a broad spectrum of hormones (Narayanan, 2020). As a result of these mechanisms, therapies to reduce androgen levels will fail to suppress CRPC (Chandrasekar, Yang, Gao, & Evans, 2015)

1.4.2 Androgen deprivation therapy

ADT is focused on reducing the levels of these androgens to prevent PCa cells from growing. Different types of ADT can be used. The most common way of ADT is by injecting drugs that lower the amount of testosterone. Another type of ADT is surgical castration. In this process, the testes, where androgens are produced, are surgically removed (Perlmutter & Lepor, 2007). A major disadvantage of ADT is that (m)HSPC can develop resistance to ADT over time. This results in (m)CRPC. To prevent this, more research is being conducted on the addition of chemotherapy or ARSIs to ADT (Dathathri et al., 2022).

1.4.3 Androgen receptor signalling inhibitors

ARSIs are novel hormone therapies, which use abiraterone and anti-androgens, such as enzalutamide and apalutamide (Mitsiades & Kaochar, 2021). Abiraterone targets CYP17. CYP17 is an enzyme which is involved in the synthesis of androgens. Abiraterone inhibits the enzymatic activities of CYP17. Enzalutamide and apalutamide are second generation anti-androgens. They both bind to the ligand-binding domain of AR, which prevents AR nuclear translocation and thus the production of androgenic proteins (Mitsiades & Kaochar, 2021)(De Velasco et al., 2021).

The addition of ARSIs and/or chemotherapy to ADT resulted in improved OS for most patients (Dathathri et al., 2022)(Wenzel et al., 2021).

Despite improved treatments for metastatic prostate cancer patients, not all patients respond similarly thereby affecting overall survival. The ineffectiveness of treatments for metastatic prostate cancer is attributed to the heterogeneity seen in the tumor of patients (Dathathri et al., 2022). To reduce the frequent administration and ineffectiveness of treatments, there is a need for prognostic markers which can help predict the response of patients to therapies, making treatments more targeted and personalized.

1.5 Aim

In this study, we aim to develop a realistic model to study the phenotypic response of PCa cell lines, towards androgen stimulation and inhibition of AR. This study will give more insight into the characteristics of different PCa cell lines, derived from different stages. These PCa cell lines can be used as models in further studies and to predict the response to treatments.

The secretion of prostate-specific antigen (PSA) was used as a read-out of the phenotypic response and validated with the identification of cellular PSA. Additionally, the expression of other biomarkers like PSMA, EPCAM and HER2 were evaluated.

To achieve this goal, the following objectives were set:

- Proteomic analysis (PSA secretion) of multiple PCa cell lines (LNCaP, PC-3, 22Rv1, RWPE-1, RWPE-2 and PWR-1E) derived from different stages of PCa, in response to androgen stimulation (R1881) and AR signalling inhibitor (Enzalutamide)
- Optimization of the quantification of PSA secretion on PDVF membranes
- Phenotypic characterization PCa cell lines (LNCaP, PC-3, 22Rv1, RWPE-1, RWPE-2 and PWR-1E)
- Culturing CTC-derived organoids from an mCRPC patient (EMC-Pca-41) and evaluating the PSA secretion

2 Materials and method

To achieve the objectives, various experiments were performed. An overview of all experiments which were performed in this project, is illustrated in Figure 3.

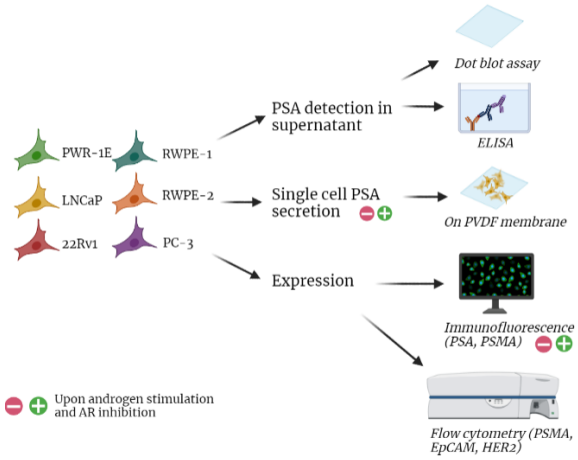

Figure 3: Methodological overview of all experiments. Created by biorender.com.

2.2 Cell lines

Different PCa cell lines derived from different stages were cultured in this project. More information about these cell lines is presented in Table 1. HEPG2 was used as a negative control cell line. The cell lines which are used (PWR-E1, RWPE-1, RWPE-2, LNCaP, 22Rv1, PC-3 and HEPG2) were obtained from American Tissue Culture Collection (ATCC, USA).

Table 1: An overview of the properties of different prostate cancer cell lines.

Cell line	Source	Metastasis	PSA secretion	Cellular PSA
Benign (Be)				
PWR-E1	Epithelial	No	No (Deep, Oberlies, Kroll, & Agarwal, 2008)	Yes (Deep et al., 2008)
RWPE-1	Epithelial	No	No (Sasaki et al., 2016)	Yes, when exposed to R1881 (Bello, Webber, Kleinman, Wartinger, & Rhim, 1997)
Hormone-sensitive (HS)				
RWPE-2	Epithelial	No	-	Yes, when exposed to R1881 (Bello et al., 1997)
LNCaP	Epithelial (lymph node)	Bone metastasis	Yes(Sasaki et al., 2016)(Yamamoto et al., 2020)(Deep et al., 2008)	Yes (Deep et al., 2008)
Castration-resistant (CS)				
22Rv1	Epithelial	Bone metastasis	Yes(Sasaki et al., 2016)(Attardi, Burgenson, Hild, & Reel, 2004)(Deep et al., 2008)	Yes (Jemaa, Sallami, Céraline, & Oueslati, 2013)
PC-3	Epithelial (vertebral)	Bone metastasis	No(Yamamoto et al., 2020)(Tai et al., 2011)	No (Tai et al., 2011)

The cells were maintained at 37°C in an atmosphere containing 5% CO_2. The components of the cell culture medium are listed in Tables 2, 3 and 4.

The cells in T25 treated culture flasks (VWR international B.V., Amsterdam, The Netherlands) were harvested when they reached 70% confluency. RWPE-1, RWPE-2, and PWR-E1 were washed

with Dulbecco's phosphate-buffered saline (DPBS) (Lonza, Verviers, Belgium). Prewarmed diluted 0.05% trypsin-EDTA (Gibco, ThermoFisher Scientific, Waltham, USA) with DPBS [1:1] was added and incubated for at least two minutes. Cells were collected in DPBS + 2% Fetal Bovine Serum (FBS) (Sigma Aldrich, St. Louis, USA) to deactivate the trypsin. The desired cell concentration was added to a new tissue culture flask with fresh cell culture medium. All three cell lines were seeded with a seeding density of 5.000 cells/cm^2.
LNCaP, PC-3 and 22RV1 cells were washed with phosphate-buffered saline (PBS) (Sigma Aldrich, St. Louis, USA). Prewarmed 0.05% trypsin-EDTA was added and incubated for 1 minute at 37ºC. When cells were detached, the cells were collected in fresh medium with pipetting and counted using the Luna-FL™ automated cell counter (Westburg B.V., Leusden, The Netherlands). The cells were passaged into new flasks and maintained in a humidified incubator at 37°C and 5% CO_2. LNCaP cells were passaged with a seeding density of 10.000 cells/cm^2, 22Rv1 with a seeding density of 5.000 cells/cm^2 and PC-3 with 2.000 cells/cm^2.
HEPG2 cells were washed with PBS. Prewarmed 0.05% trypsin-EDTA was added and incubated for 5 minutes. Cell culture medium was added to neutralize the trypsin. With a seeding density of 5.000 cells/cm^2, the cells were passaged to a new tissue culture flask with fresh medium.

The cell culture medium was replaced every 3-4 days for all cell lines.
For the PSA secretion experiments LNCaP cells were cultured from passages p.41 to p.45, PC-3 from p.98 to p.102, RWPE-1 p.65 to p.69, RWPE-2 p.67 to p.75, PWR-E1 px+4 to px+11, 22Rv1 px+7 to px+11. For the immunofluorescence staining passage numbers LNCaP p.52, PC-3 p.109, RWPE-1 p.76, RWPE-2 p.77, PWR-E1 px+12, 22Rv1 px+21 are used. For the expression experiments LNCaP p.43, PC-3 p.100, RWPE-1 p.67, RWPE-2 p.68, PWR-E1 px+4, 22Rv1 px+9 are used. LNCaP p.52, PC-3 p.109, RWPE-1 p.76, RWPE-2 p.77, PWR-E1 px+12, 22Rv1 px+21 are used. Supernatant for PSA secretion experiments is stored from the following passage numbers of the cells LNCaP p.53, PC-3 p.112, RWPE-1 p.77, RWPE-2 p.81, PWR-E1 px+13, 22Rv1 px+26.

Table 2: Cell culture medium components PWR-E1, RWPE-1 and RWPE-2.

Reagent	Concentration in media	Stock concentration	Catalogue number	Supplier
Keratinocyte serum-free medium (SFM)	-	500 mL	17005042	Gibco
human epidermal growth factor (EGF)	5 ng/ml	2.5ug/ml	10450-013	Gibco
bovine pituitary extract (BPE)	50 µg/ml	25mg/ml	13028-014	Gibco

Table 3: Cell culture medium components of LNCaP, 22Rv1 and PC-3 cells

Reagent	Concentration in media	Stock concentration	Catalogue number	Supplier
Roswell Park Memorial Institute (RPMI 1640)	-	500 mL	BE12-702F	Lonza
Fetal Bovine Serum (FBS)	10%	-	F7524	Sigma Aldrich
Penicillin/streptomycin	100 u and 100 µg/mL	10.000 u and 10.000 µg/ml	Cat. DE17602E	Lonza
L-Glutamine	2 mM	200 mM	Cat. Be17605E	Lonza

Table 4: Cell culture medium components of HEPG2 cells.

Reagent	Concentration in media	Stock concentration	Catalogue number	Supplier
Dulbecco's modified Eagle's medium (DMEM)	-	500 mL	41965-039	Gibco, ThermoFisher Scientific
Fetal Bovine Serum (FBS)	10%	-	F7524	Sigma Aldrich
Penicillin/streptomycin	100 u and 100 µg/mL	10.000 u and 10.000 µg/ml	Cat. DE17602E	Lonza

2.2 Organoid culture

Circulating tumor cells (CTCs) are interesting cells for individualised disease modelling as they reflect phenotypic and genotypic heterogeneity of the tumor (Dathathri et al., 2022)(Mout et al., 2021). The number of CTCs is associated with prognostic values. CTCs can be obtained from mPCa patients by DLA and can be cultured as organoids. These organoids are a more representative model of the disease than standard 2D cell lines. However, the success rate of generating organoid cultures derived from CTCs is very low. In the study of L. Mout et all, one stable CTC-derived organoid cell line (EMC-PCa-41) from an mCRPC patient is generated out of 40 DLA samples (Mout et al., 2021). The organoid cell line EMC-PCa-41 was cultured in this project.

The organoid cell line EMC-PCa-41 (kindly provided by Erasmus MC, Rotterdam, The Netherlands) was used. Cells were thawed and collected by centrifugation at 1200 g for 5 minutes at 4ºC. On ice, Cultrex Reduced Growth Factor Basement Membrane Extract (RGF BME) Type R1 (R&D systems, Bio-Techne, Minneapolis, USA) (Matrigel) was added to the cell pellet (Ratio cell suspension: Matrigel is 1:3). Droplets of 30µL were made in a pre-warmed 24-wells plate (VWR international B.V., Amsterdam, The Netherlands). Next, the plate was incubated for 30 minutes upside-down at 37ºC and 5% CO_2. Subsequently, 500µL of adjusted prostate cancer organoid medium (APCOM medium) was added. The components are listed in Table 2. The cell culture medium was replaced every 2-3 days. The organoids were passaged once a month after they were brought into culture.

For passaging or obtaining single cell suspension, the organoid cells were mechanically disrupted. They were resuspended in Advanced DMEM/F12 + Non-Essential Amino Acids + 110 mg/L Sodium Pyruvate + L-Glutamide (Gibco, ThermoFisher Scientific, Waltham, USA), supplemented

with HEPES (ThermoFisher Scientific, Waltham, USA) and pen/strep (AdMEM/F12+++). The collected cells were centrifuged at 1200g for 5 min and plated as described previously. Another method that was used to passage the organoids was with the use of trypsin. TryplE (Gibco, ThermoFisher Scientific, Waltham, USA) was added to the wells and incubated for 20-30 minutes at 37ºC. The cell suspension was resuspended and trypsin inhibiter (Merck, Sigma Aldrich, USA) (ratio 1:1) was added. Subsequently, this cell suspension was collected in AdMEM/F12 +++ medium to wash the cells. After washing, the cells were plated as described previously.

To evaluate the cell viability, calcein [4µM] (Invitrogen, ThermoFisher Scientific, Waltham, USA) was incubated for 30 minutes in one well with organoid cells in Matrigel. Hoechst [, 4µg/mL] (Invitrogen, ThermoFisher Scientific, Waltham, USA) was incubated for the last 10 minutes. With an inverted fluorescence microscope (Nikon, Eclipse Ti, Minato, Japan), the cells were imaged.

Table 1: Components of Adjusted Prostate Cancer Organoid Medium (APCOM)

Reagent	Concentration in media	Stock concentration	Catalogue number	Supplier
Advanced DMEM/F12		500 mL	12634010	ThermoFisher Scientific
HEPES	10 mM	1M	15630080	ThermoFisher Scientific
L-Glutamine	2 mM	200 mM	Cat. Be17605E	Lonza
Penicillin/streptomycin	100 u and 100 µg/mL	10.000 u and 10.000 µg/ml	Cat. DE17602E	Lonza
Noggin	0.1ug/ml	200ug/ml	120-10C	Peprotech
R-spondin	0.5ug/ml	500ug/ml	120-38	Peprotech
Epithelial growth factor (EGF)	20 ng/mL	1mg/ml	E-9644	Sigma-Aldrich
Fibroblast growth factor 2 (FGF-2)	5 ng/mL	100ug/ml	233-FB-025	R&D Systems
Fibroblast growth factor 10 (FGF-10)	10 ng/mL	50ug/ml	100-26	PeproTech
A-83-01	500 nM	25mM	2939	Tocris Bioscience
Prostaglandin Ed (PGE2)	0,5 µM	100mM	1254	Tocris Bioscience
Y-27632 dihydrochloride	10 µM	100mM	1254	Abmole Bioscience
Metribolone R1881	5nM	20mM	Lot #041015	Biotangusa

2.3 Immunofluorescence staining and imaging

One flask of each cell line was stimulated with R1881 [0.5ng/mL] (TSZCHEM, Wadeville, South Africa) overnight. The next day, 100.000 cells were seeded in a 24 well plate (VWR international B.V., Amsterdam, The Netherlands) and R1881 [0.5ng/ml] or Enzalutamide [2µg/ml] (MDV3100, Selleckchem, Houston, USA) was added. Enzalutamide was added to the wells with R1881 stimulated cells (stimulated overnight), as illustrated in Figure 4. The well plate was incubated for 24 hours and 48 hours at 37ºC and 5% CO_2. Subsequently, the cells were fixed with 1% formalin

(Sigma Aldrich, St. Louis, USA). The cells were permeabilized by washing with 0.1% Triton X-100 (Sigma Aldrich, St. Louis, USA) in PBS for 15 minutes. Next, the cells were washed twice with PBS and after that 1% Bovine Serum Albumin (BSA) (Sigma Aldrich, St. Louis, USA) in PBS was added for 30 minutes.

For staining, a primary antibody (Rabbit to PSA Ab, Cat. 19554, Abcam, Cambridge, UK) was prepared [2µg/mL] in 0.1% BSA in PBS and incubated for 60 minutes. The membranes were washed with PBS. A secondary antibody solution was prepared [2µg/ml] (Goat pAb to Rb IgG, Alexa Fluor 488, Cat. 150077, Abcam, Cambridge, UK) in 0.1% BSA in PBS including a PSMA-PE antibody (FOLH1) [1 µg/ml] (Cat. 342504, BioLegend, San Diego, USA).

After washing with PBS, DAPI [4 µM] (CellSearch, Menarini Silicon Biosystems, Bologna, Italy) was added to the wells and incubated for 15 minutes. The wells were washed with PBS and stored in PBS at 4ºC. With a fluorescence microscope (Nikon, Eclipse Ti, Minato, Japan), the cells were imaged. In the DAPI channel, an exposure time of 50 millisecond (ms) was used and in FITC and PE channels an exposure time of 200 ms was used.

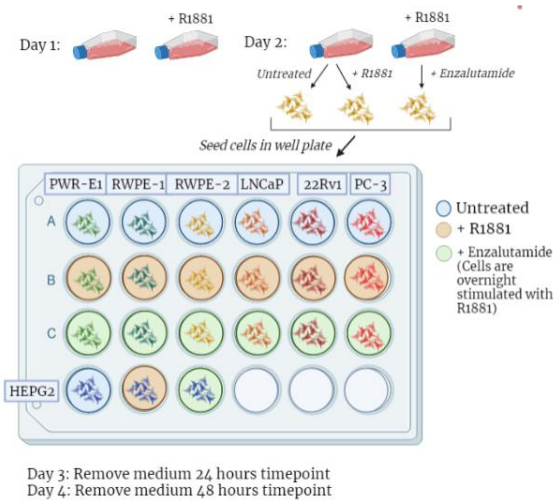

Figure 4: An illustration of the different prostate cancer cell lines seeded in the wells plate in three conditions. On day 1, 1 flask was stimulated with R1881. On day 2, the cells were seeded in a well plate. The cells of the untreated flask were split into two cell suspensions. One part remained untreated, the other part was stimulated with R1881. Enzalutamide was added to the overnight R1881 treated flask. Blue wells: untreated cells. Orange wells: Cells are androgen stimulated with 0.5nM R1881. Green wells: Cells are treated with 2µM Enzalutamide, after overnight incubation with 0.5nM R1881. The well plate is in duplicate for the 24-hour and 48-hour timepoint. Created by biorender.com.

2.4 PSA detection in the supernatant (dot blot)

To detect PSA in the supernatant of cell lines, the supernatant of all cell lines was stored after 7 days of passaging, excluding RWPE-1 and HEPG2. The supernatant of these cell lines was stored after 24 hours and 48 hours after passaging.

Polyvinylidene fluoride (PVDF) membranes (Immun-Blot, 0.45 µm pore size) (BIO-Rad Laboratories B.V., Veenendaal, the Netherlands) membranes were incubated with methanol for 1 minute and washed with PBS. Droplets of 2 µL of the supernatant were added to the membrane. Next, the membranes were blocked using 3% BSA in PBS for 30 minutes. Subsequently, the staining protocol, as mentioned in 2.5.3 was performed.

2.5 Capturing PSA secretion on membranes from PCa cell lines

A schematic overview of the methodology to capture PSA secretion from the PCa cell lines on PVDF membranes is illustrated in Figure 5.

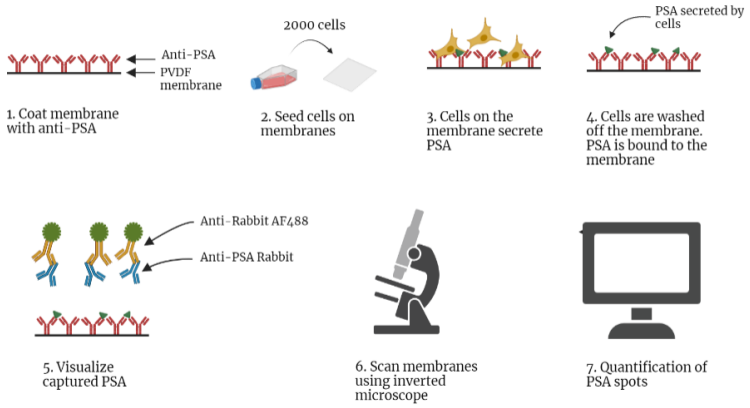

Figure 5: A schematic overview of capturing PSA secretion on membranes. Created by biorender.com.

2.5.1 Preparation of the PVDF membranes

Under sterile conditions, PVDF membranes (Immun-Blot, 0.45 µm pore size) (BIO-Rad Laboratories B.V., Veenendaal, the Netherlands) were placed in a 24-wells plate (VWR international B.V., Amsterdam, The Netherlands) and incubated with methanol (100%) for 1 minute. Membranes were washed twice with 1X PBS. Subsequently, a monoclonal mouse anti-PSA antibody solution (Cat.10-P21A, Fitzgerald Industries International, Acton, USA) with a concentration of 25µg/mL in 1x PBS was prepared and added to the membranes. The membranes were incubated overnight at 4ºC. The next day the antibody solution was removed and a 3% BSA in 1X PBS solution was added to block the membranes for 1 hour. Membranes were washed with 1X PBS.

2.5.2 Capturing PSA secretion from PCa cell lines

One flask of each cell line was stimulated with R1881 [0.5ng/mL] overnight. The next day 2000 cells were seeded on the membranes and R1881 [0.5ng/mL] or Enzalutamide [2µg/ml] was added to the cells on the membranes. Enzalutamide was added to the membranes with R1881 stimulated cells (overnight stimulation). A schematic overview of the method to seed cells on a membrane, is shown in Figure 4. The membranes were incubated at 37ºC and 5% CO_2. After the first 24 hours, the medium cell culture medium was removed from half of the membranes and these membranes were washed with 1% Tween 80 (Sigma Aldrich, St. Louis, USA) in PBS for 30 minutes on a thermoshaker (Thermomixer C, Eppendorf, Hamburg, Germany) at 300 rpm to wash the cells off. This was followed by washing with 1% BSA in PBS for 30 minutes on the thermoshaker at 300 rpm. After 48 hours of incubation, the other half of the membranes underwent the same steps.

2.5.3 Detection of PSA

To visualize the PSA which is captured on the membranes, a primary antibody [2µg/mL] (Rabbit to PSA Ab, Cat. 19554, Abcam, Cambridge, UK) was diluted in 1% BSA in PBS. The antibody solution was added to the membranes and placed on the thermoshaker for 1 hour at 300 rpm. The membranes were washed three times for 5 minutes with 1% BSA in PBS. Subsequently, a secondary antibody was prepared [2µg/ml] (Goat pAb to Rb IgG, Alexa Fluor 488, Cat. 150077, Abcam, Cambridge, UK) in 1% BSA in PBS. The antibody solution was added to the membranes and placed on the thermoshaker for 1 hour at 300 rpm. Again, the membranes were washed three times for 5 minutes with 1% BSA in PBS. The stained membranes were dried and placed between two microscope slides. Using the VyCAPs scan program the membranes were imaged using an inverted microscope (Nikon, Eclipse Ti, Minato, Japan) in the FITC channel using an exposure time of 20 ms, with a 10x objective. Around 10x10 images were acquired. A montage of these images was made using Image J software and saved in tiff format.

Due to a change in the optical fibre of the microscope the images of the first experiments were imaged with an exposure time of 50 ms. In Supplementary Table 1, an overview of all datasets and their properties is shown.

2.5.4 Calibration curve

A serial dilution (0-300 µg/mL) of the Prostate Specific Antigen peptide (Cat. no. ab41421, Abcam, Cambridge, UK) was prepared and droplets of 2 µL of each concentration were spotted in triplicates on the PVDF membranes. PSA was detected as mentioned in Section 2.5.2. The spots were analysed using the Image J software. The mean intensity and the size of each spot were determined. The amount of PSA present in one spot was divided by the area of the spot to calculate the amount of PSA in pg/µm^2. The different amounts of PSA in pg/µm^2 versus the mean intensity were plotted. To determine the amount of PSA secreted by a cell, the amount of PSA in pg/µm^2 was multiplied by the area of the spot. The amount of PSA pg/µm^2 can be read out in the calibration curve using the mean intensity of the spot.

2.5.5 Quantification

The quantification was done using the Image J software. A montage of the individual images was made and saved as a TIFF file. The image was duplicated and the duplicated image was saved as a 10-bit image. Then a threshold was set on the duplicated image with a minimum pixel intensity of 550. A binary image was created and linked to the original image. The area and the mean intensity of the regions of interest were computed. The values of the mean intensity were normalized to the membranes of the HEPG2 cells. A more detailed protocol, with some exceptions, is presented in the Supplementary Data.

2.6 Enzyme-linked immunosorbent assay

A monoclonal mouse anti-PSA antibody solution [25µg/mL] (Cat.10-P21A, Fitzgerald Industries International, Acton, USA) in 1x PBS was prepared and used to coat a 96 microwell immuno plate (172164, Sigma Aldrich, St. Louis, USA). This capture antibody was incubated overnight. The next day, the wells were washed with 1% Tween 20 (Sigma Aldrich, St. Louis, USA) and 1% BSA in PBS was incubated for 1 hour. The samples of interest were diluted in 1% BSA and 5% FBS in PBS and samples for a calibration curve were prepared. For the calibration curve serial dilutions of the Prostate Specific Antigen peptide (Cat. no. ab41421, Abcam, Cambridge, UK) were made from 0 to 60 ng/ml. Only LNCaP samples were diluted as described in Table 5.
The wells were washed again and the diluted samples and the samples for the calibration curve were incubated (100 µL/well) for 2 hours. Next, a primary antibody [2µg/mL] ((Rabbit to PSA Ab,

Cat. 19554, Abcam, Cambridge, UK) was prepared in 1% BSA in PBS and incubated for 1 hour. The wells were washed again and an anti-rabbit-HRP [3 µg/ml] (Dako, Agilent, Santa Clara, USA) solution in 1% BSA in PBS was prepared and incubated for 20 minutes in the dark. The wells were washed again and streptavidin (Lot.P300867, R&D systems, Minneapolis, USA)) diluted in 1% BSA in PBS [dilution1:40] was added. After washing 1-Step™ Ultra TMB-ELISA Substrate Solution (Thermo Scientific, ThermoFisher Scientific, Waltham, USA) was incubated until a clear difference in different shades of blue was visible in the standard. Subsequently, 1.8M H_2SO_4 (Sigma Aldrich, St. Louis, USA) in MilliQ was prepared and added to the wells. The absorbance was measured using a VictorX3 microplate reader (PerkinElmer, Waltham, USA).

Table 5: Dilution factors of ELISA samples

Cell line	Conditions	Dilution factor
LNCaP	Supernatant is collected after 7 days. On day 7 an 80% confluency. T25 flask.	100x
LNCaP	100.000 cells seeded in a 24-wells plate. Stimulated with R1881. Supernatant is collected after 48 hours.	400x

2.7 Flow cytometry

100.000 cells were collected in a tube and fixed using 1% formalin in PBS for 15 minutes. The cells were washed with PBS. The cells were centrifuged for 5 minutes at 500 Relative Centrifugal Force (RCF). The supernatant was aspirated and the cell suspension samples were divided into different samples. To each sample, 100 µL of different primary antibody solutions were added. The different primary antibody solutions were HER2/neu [1µg/ml] (Immunicon, Huntingdon Valley, USA), VU1D9 [1µg/ml] (Veridex), and Purified anti-human PSMA (FOLH1) (Cat. 342502) [10µg/ml] (BioLegend, San Diego, USA).

The primary antibodies were incubated at 37°C for 30 minutes. Cells were washed with 1% BSA in PBS. A secondary antibody solution (F(ab')2-Goat anti-Mouse IgG (H+L), PE) [2.5µg/ml] (FisherScientific, ThermoFisher Scientific, Waltham, USA) was prepared, added to each sample and incubated at 37°C for 30 minutes. Cells were washed with 1% BSA in PBS. The samples were measured with the FACS device (BD Bioscience, Franklin Lakes, USA). BD Quantibrite™ PE (BD Bioscience, Franklin Lakes, USA) were used to make a standard curve.

2.8 Graphs and statistical analysis

The graphs were created using the software GraphPad Prism (Version 5, GraphPad Software, San Diego, USA). Statistically significant differences between the two conditions were determined using Student's t-test. Differences with P-values of < 0.05 were considered statistically significant. * $0.05 < P$ **$0.01 < P$ ***$0.001 < P$

3 Results and discussion

3.1 EMC-PCa-41 organoids

The EMC-PCa-41 organoids were thawed and plated in Matrigel as mentioned in Section 2.3, see Figure 6. The EMC-PCa41 organoids were kept in Matrigel and observed for growth. The growth of cells was very slow and no organoid formation was visible for four weeks. The cells were passaged and re-seeded in new Matrigel.

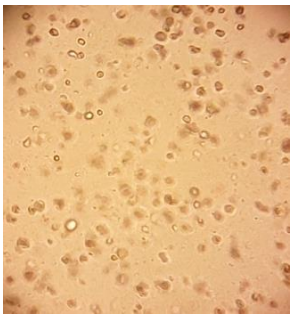

Figure 6: An image of EMC-PCa-41 cells after thawing and plating in Matrigel in a wells plate.

Immunofluorescence staining was performed to visualize the presence of PSA protein, PSMA surface marker and the nucleus. The immunofluorescence staining showed the presence of no cells. This could indicate that most cells were dead and lost during the staining protocol. Cell counting also showed the presence of no cells, hence viability (trypan blue) staining could not be performed to confirm the presence of live cells during passaging.

To check for viability, Calcein and Hoechst staining were performed. Only a few cells were visualized, as shown in Figure 7. Calcein staining was not observed, indicating the absence of live cells.

The supernatant of the EMC-PCa-41 cells was stored every month consecutively to check for the presence of PSA protein in the supernatant. These results are described in Section 3.3.

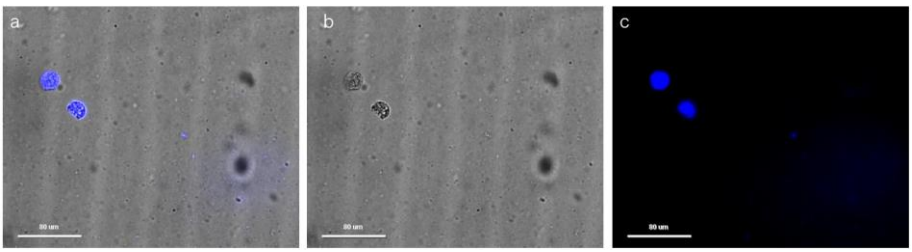

Figure 7: Images of EMC-PCa-41 organoid cells in Matrigel, 14 weeks after thawing. The cells are stained with Calcein and Hoechst (blue, DAPI). a) Merge of Bright field and Hoechst, b) Bright field, c) Hoechst. Calcein is not observed, indicating the absence of life cells. Exposure time is 250 ms. Scale bar: 80 µm.

We did not succeed to culture EMC-PCa-41 organoids. This could be due to different reasons. A month after thawing, the organoids were passaged for the first time. Earlier passaging of the organoids might have led to higher stability of the Matrigel and perhaps a more optimal environment for the organoid cells. Besides, after passaging the organoids, a lower cell density was observed. The lack of cell-cell contact could complicate the ability to generate organoids. Lastly, culturing CTC-derived prostate cancer organoids can be very challenging. In the study of L. Mout et al., 14 CTC derived organoids were established out of 40 DLA samples. However, only two organoid cultures could be maintained for over six passages (Mout et al., 2021). It might be that the current culture techniques do not provide an optimal environment for sustained viability. Nevertheless, we cannot explain why we did not succeed to culture the EMC-PCa-41 organoids.

3.2 Phenotypic characterization of prostate cancer cell lines in response to drugs

The immunofluorescence staining of prostate cancer cell lines was performed with anti-PSA (Alexaflurophore AF488), antiPSMA (PE) and DAPI to visualize the presence of PSA protein, PSMA surface marker and the nucleus respectively. Additionally, the cells were androgen stimulated for 24 hours with R1881 and AR inhibited with Enzalutamide, as described in Section 2.3. The phenotypic assessment of the following prostate cancer cell lines is shown below.

3.2.1 PWR-E1 (benign)

The PWR-1E cells showed a monolayer of cells and appear healthy and stretched (Figure 8).

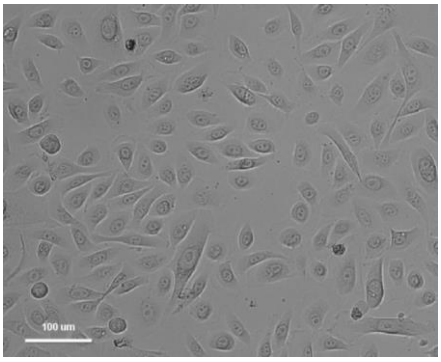

Figure 8: A bright field image of PWR-E1 cells. Cells show a stretched morphology. Scale bar: 100 µm.

The immunofluorescent images of PWR-1E cells (Figure 9) show the presence of intracellular PSA protein in the three conditions (untreated, androgen stimulated, and AR inhibited). However, PSA protein is not expected throughout the nucleus of the cell. The presence of unspecific staining in the nucleus of the cells is indicated with red arrows in Figure 9i. Specific staining of PSA in the cytoplasm is indicated by green arrows as shown in Figure 9g,i. A possible reason for the unspecific staining can be attributed to the non-specific binding of the secondary antibody to the cell nucleus. To confirm this, the primary antibody in a next experiment should be absent.

No PSA protein was observed in the cytoplasm of the untreated and androgen stimulated cells (Figure 9 a,c,d,f). However, our results indicate the presence of the PSA protein after treatment with Enzalutamide (Figure 9 g,i). This is contradictory to findings in the literature. Literature indicates also the presence of cellular PSA in untreated PWR-E1 cells using western blot (Deep et al., 2008). These experiments must be repeated to confirm these contradictory findings.

PSMA expression was not observed in the PWR-1E cell line. No other research is done into PSMA expression in PWR-1E cells.

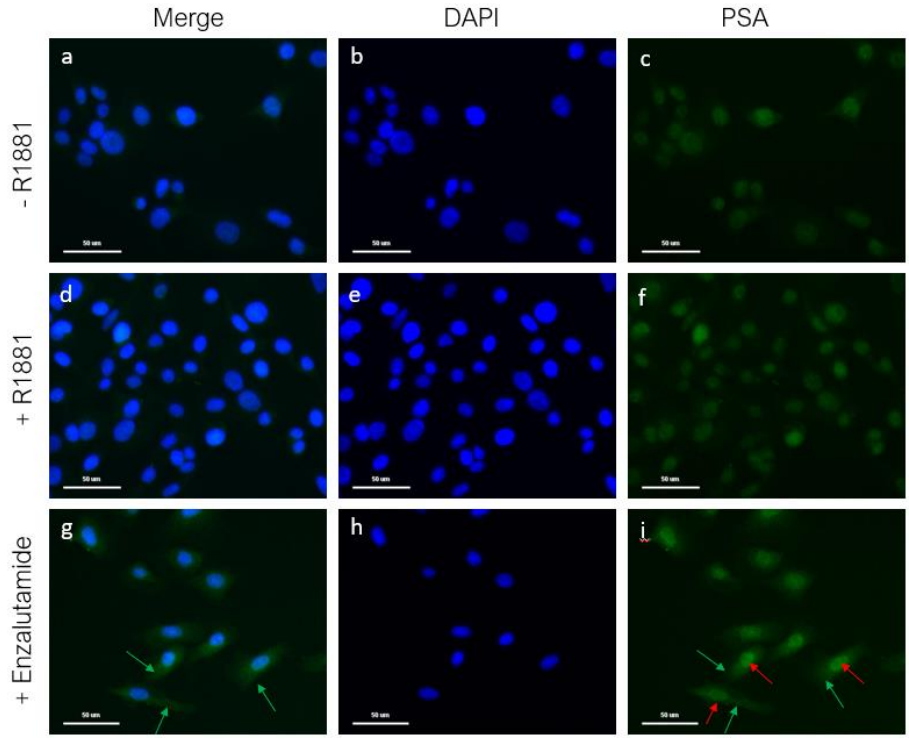

Figure 9: Immunofluorescence detection of both PSA and PSMA expression in PWR-E1 cells following androgen stimulation (R1881) or Enzalutamide treatment. Cell nuclei were counterstained with DAPI (blue). A,b,c) Untreated PWR-E1 cells. d,e,f) Androgen stimulated (R1881) PWR-E1 cells. F,h,i) Enzalutamide treated PWR-E1 cells. Specific fluorescence signals for PSA (green) were detected, indicated by the green arrows. Fluorescence signals for PSA throughout the nuclei (red arrows) are not indicated as true PSA expression. No signals for PSMA were detected in PWR-E1 cells (not shown). Scale bar: 50 µm

3.2.2 RWPE-1 (benign)

The immunofluorescent images of RWPE-1 cells are shown in Figure 10. Figure 10 (a,c,d,f,g,i) indicated the absence of PSA protein in the cytoplasm in all three conditions (untreated, androgen stimulated and AR inhibited).

From the clinic is known that benign prostate cells secrete in general lower PSA levels than cancerous prostatic cells (Tikkinen et al., 2018). This is in accordance with our results. We did not identify PSA expression in the benign RWPE-1 cell line.

However, the study of D. Bello et all reported PSA expression in RWPE-1 cells after 6 days of treatment with mibolerone, a non-metabolizable androgen (Bello et al., 1997). This is contradictory to our findings. This may be due to the different stimulation compounds and stimulation time.

PSMA expression was not observed in RWPE-1 cells. This is in accordance with the literature, as RWPE-1 is classified as a benign and a PSMA-negative cell line (Tse et al., 2015).

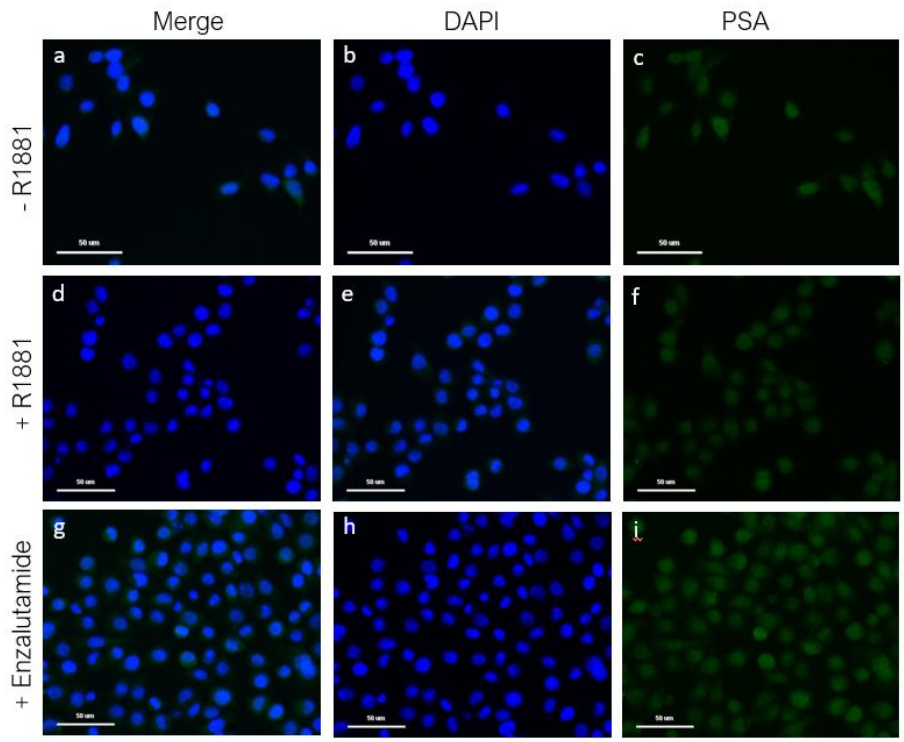

Figure 10: Immunofluorescence detection of both PSA and PSMA expression in RWPE-1 cells following androgen stimulation (R1881) or Enzalutamide treatment. Cell nuclei were counterstained with DAPI (blue). A,b,c) Untreated RWPE-1 cells. d,e,f) Androgen stimulated (R1881) RWPE-1 cells. F,h,i) Enzalutamide treated RWPE-1 cells. Specific fluorescence signals for PSA (green) were not detected outside the nuclei. No signals for PSMA were detected in RWPE-1 cells (not shown). Scale bar: 50 µm

3.2.3 RWPE-2 (hormone-sensitive)

The RWPE-2 cells appeared stellated shaped with some long cytoplasmic processes (Figure 11).

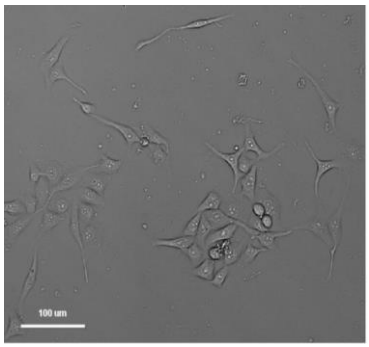

Figure 11: A bright field image of RWPE-2 cells. Cells show a stretched morphology. Scale bar: 100 µm.

The immunofluorescent staining on RWPE-2 cells indicated increased cellular PSA expression after androgen stimulation, as shown in Figure 12 (a,c,d,f).

This is in accordance with the article of D. Bello et al.. This study detected no PSA expression in untreated cells, but observed PSA expression in RWPE-2 cells after 6-day of treatment with androgen mibolerone (Bello et al., 1997).

Figure 12 suggests low levels of PSA expression in untreated hormone-sensitive RWPE-2 cells, elevated PSA expression levels after androgen stimulation and again low PSA expression levels when the cells are AR inhibited using Enzalutamide. This is in line with expectations of a hormone-sensitive cell line. Hormone-sensitive PCa patients react to hormone therapies, like enzalutamide, which results in lower PSA levels (Perlmutter & Lepor, 2007).

PSMA is highly expressed in PCa cells. However, PSMA expression is heterogeneous and some patients and PCa cell lines lack PSMA expression (Sheehan et al., 2022). This is in accordance with our results. PSMA expression was not observed in the hormone-sensitive cell line RWPE-2. Our results suggest that RWPE-2 is a PSMA negative cell line.

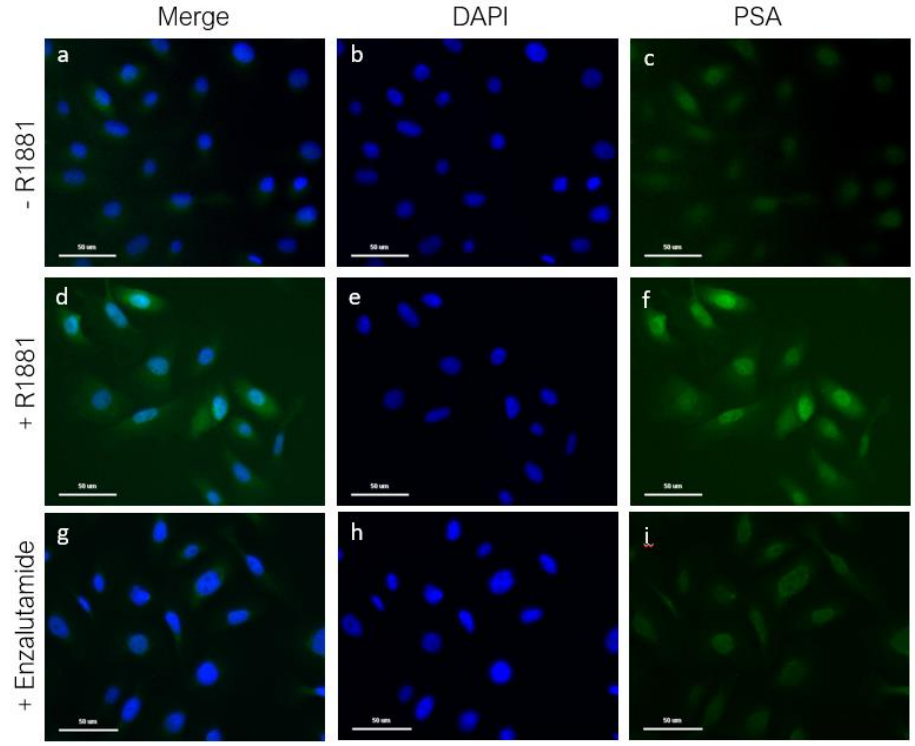

Figure 12: Immunofluorescence detection of both PSA and PSMA expression in RWPE-2 cells following androgen stimulation (R1881) or Enzalutamide treatment. Cell nuclei were counterstained with DAPI (blue). A,b,c) Untreated RWPE-2 cells. d,e,f) Androgen stimulated (R1881) RWPE-2 cells. F,h,i) Enzalutamide treated RWPE-2 cells. Specific fluorescence signals for PSA (green) were detected outside the nuclei. Upon androgen stimulation a higher signal of PSA is detected. No signals for PSMA were detected in RWPE-2 cells (not shown). Scale bar: 50 µm

3.2.4 LNCaP (hormone-sensitive)

The LNCaP cells showed a monolayer of stellate shaped cells and appeared stretched (Figure 13).

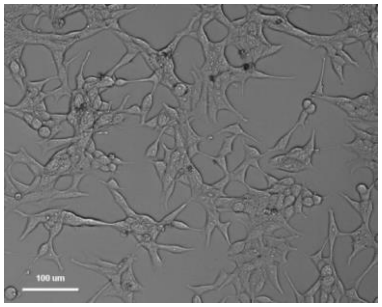

Figure 13: A bright field image of LNCaP cells. Cells show a stellate-shaped morphology. Scale bar: 100 µm.

The images of the immunofluorescence staining in LNCaP cells are shown in Figure 14. Figure 14 (c,d,g,h,k,l) indicates that in all three conditions PSA, as well as, PSMA was expressed. This is in accordance with findings in the literature. Results by T.M. gorges et all. and B. Sheehan et all. observed PSMA expression using immunofluorescence staining in LNCaP cells (Gorges et al., 2016)(Sheehan et al., 2022). Other studies reported PSA expression in LNCaP cells using techniques such as immunohistochemistry (IHC) and western blot (Sasaki et al., 2016) (Deep et al., 2008).

The androgen stimulated cells indicated elevated PSA expression (Figure 14 g) and the AR inhibited cells indicated lower PSA expression (Figure 14 k). This is in line with findings in the literature. The same effect of androgen stimulation and AR inhibition on PSA secretion is observed in other studies (Abali et al., 2021). This is also in line with expectations of a hormone-sensitive cell line. Hormone-sensitive PCa patients react to hormone therapies, like enzalutamide, which results in lower PSA levels (Perlmutter & Lepor, 2007).

Our results observed the presence of the PSMA protein in the hormone-sensitive LNCaP cell line. In addition, our results indicated elevated PSMA expression levels after androgen stimulation, compared to the untreated cells (Figure 14 d,h) and the similar PSMA levels of untreated LNCaP cells and AR inhibited LNCaP cells. This is contradictory with the study of M. Staniszewska et al.. This study observed elevated PSMA levels in LNCaP cells after treatment with enzalutamide (Staniszewska et al., 2021). These differences must be interpreted with caution because, in the study of M. Staniszewska et al. LNCaP cells were treated with 10µM Enzalutamide for at least one week. In our study, LNCaP cells were treated with 2 µM Enzalutamide for 24 hours.

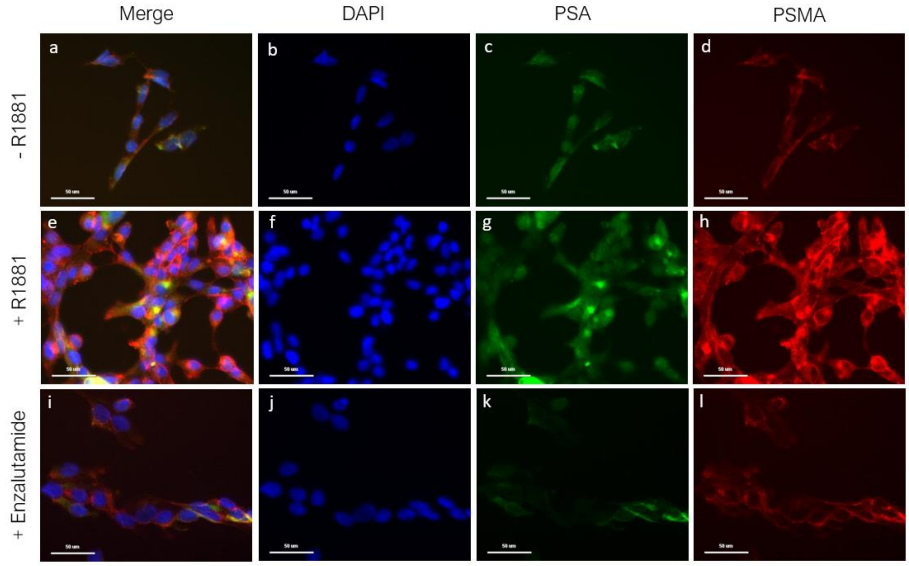

Figure 14: Immunofluorescence detection of both PSA and PSMA expression in LNCaP cells following androgen stimulation (R1881) or Enzalutamide treatment. Cell nuclei were counterstained with DAPI (blue). A,b,c,d) Untreated LNCaP cells. e,f,g,h) Androgen stimulated (R1881) LNCaP cells. I,j,k,l) Enzalutamide treated LNCaP cells. Specific fluorescence signals for PSA (green) and PSMA (red) were detected outside the nuclei. Upon androgen stimulation, a higher signal of PSA and PSMA is detected. Scale bar: 50 µm

3.2.5 22Rv1 (castration-resistant)

The 22Rv1 cells showed an epithelial rectangular shaped morphology. Most of the cells were clustered together (Figure 15)

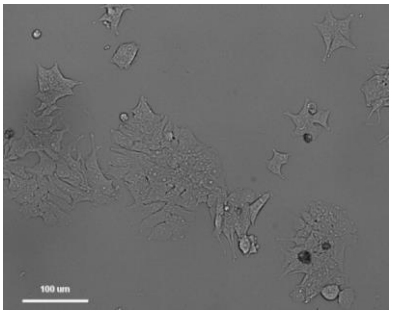

Figure 15: A bright field image of 22Rv1 cells. Cells show an epithelial rectangular-shaped morphology. Scale bar: 100 µm.

The immunofluorescence images in figure 16 showed the presence of the PSA and PSMA protein in the 22Rv1 cell line, under different conditions. Only very low levels of PSA expression were detected in androgen stimulated 22Rv1 cells, which is contradictory to findings in the literature. Previous studies showed PSA expression of untreated 22Rv1 cells using techniques such as western blot (Sasaki et al., 2016)(Deep et al., 2008). These experiments must be repeated to confirm these contradictory findings.

High expression of PSMA is expected in castration-resistant cell lines, but due to PSMA heterogeneity, this differs per cell line and patient. Our results indicated low levels of PSMA expression in a subpopulation of the 22Rv1 cells. These findings follow a similar observation with the literature. T.M. Gorges reported less than 30% PSMA positive 22Rv1 cells and M. Staniszewska et al., showed around 20% PSMA positive 22Rv1 cells (Gorges et al., 2016)(Staniszewska et al., 2021).

Comparable PSMA expression levels were detected in the untreated and androgen stimulated cells (Figure 16 d,h). However, no PSMA was detected in the AR inhibited 22Rv1 cells (Figure 16 l). This is contradictory to findings in the literature. The study of M. Staniszewska et al. indicated

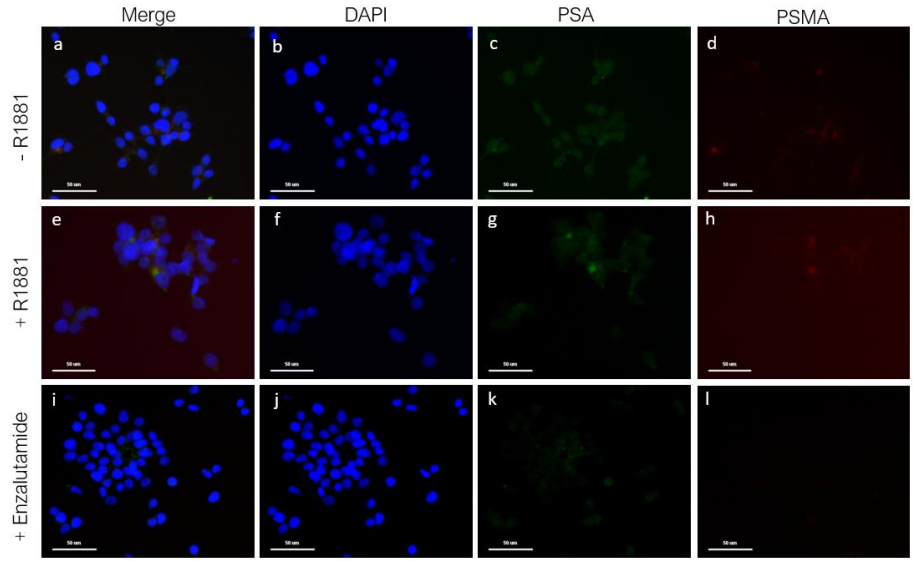

Figure 16: Immunofluorescence detection of both PSA and PSMA expression in 22Rv1 cells following androgen stimulation (R1881) or Enzalutamide treatment. Cell nuclei were counterstained with DAPI (blue). A,b,c,d) Untreated 22Rv1 cells. e,f,g,h) Androgen stimulated (R1881) 22Rv1 cells. I,j,k,l) Enzalutamide treated 22Rv1 cells Specific fluorescence signals for PSA (green) and PSMA (red) were detected minimal outside the nuclei upon androgen stimulation. Scale bar: 50 µm

increased PSMA levels after treatment with enzalutamide. These differences must be interpreted with caution because in the study of M. Staniszewska et al., 22Rv1 cells are treated with 10µM Enzalutamide for one until three weeks (Staniszewska et al., 2021). In our study, 22Rv1 cells were treated with 2 µM Enzalutamide for 24 hours. These experiments must be repeated under the same conditions to confirm these contradictory findings.

3.2.6 PC-3 (castration-resistant)

The PC-3 cells showed a monolayer of stellate shaped cells with some long cytoplasmic processes (Figure 17).

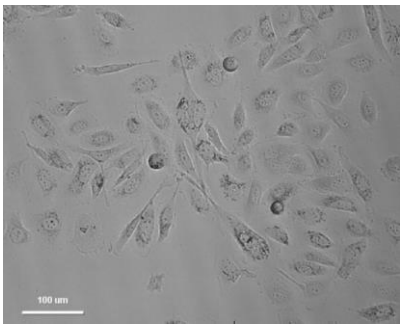

Figure 17: A bright field image of PC-3 cells. Cells *are* *µm.*

No PSA expression was observed in castration-resistant PC-3 cells (Figure 18 c,f,i), which is in accordance with the literature. It is well known that PC-3 cells do not express PSA (Tai et al., 2011)(Yamamoto et al., 2020).

This is not in line with the fact that most mCRPC patients have elevated PSA levels. However, there

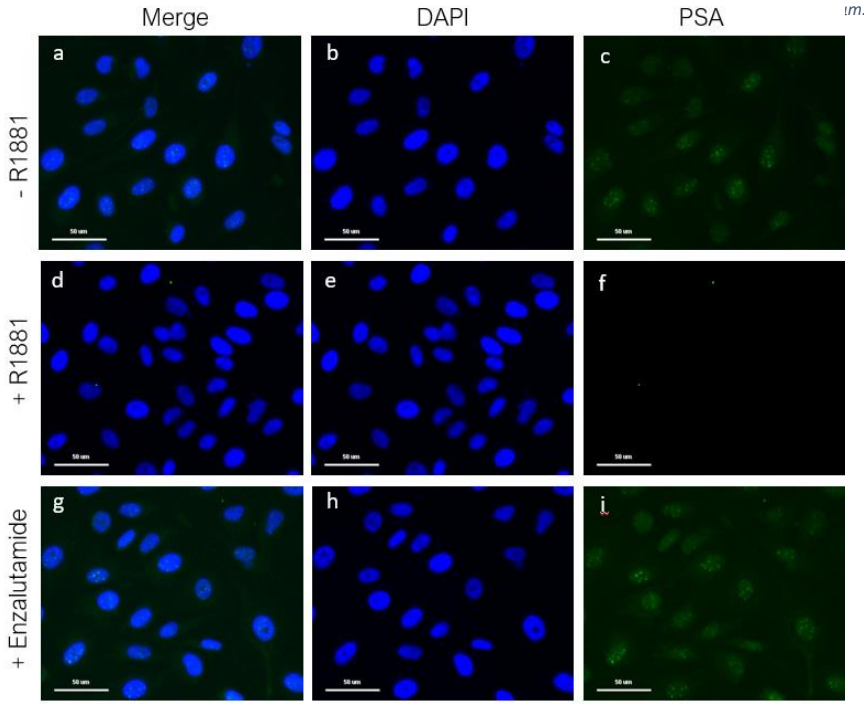

Figure 18: Immunofluorescence detection of both PSA and PSMA expression in PC-3 cells following androgen stimulation (R1881) or Enzalutamide treatment. Cell nuclei were counterstained with DAPI (blue). A,b,c) Untreated PC-3 cells. d,e,f) Androgen stimulated (R1881) PC-3 cells. F,h,i) Enzalutamide treated PC-3 cells. Specific fluorescence signals for PSA (green) were not detected outside the nuclei. No signals for PSMA were detected in PC-3 cells (not shown). Scale bar: 50 µm.

exceptions and some aggressive mCRPC tumours have also low PSA levels (Tikkinen et al., 2018)(Carm et al., 2019).

In addition, no PSMA staining was observed in PC-3 cells, which is in accordance with the literature (Laidler, Dulińska, Lekka, & Lekki, 2005). As previously described, PSMA is generally expressed in mCRPC patients. However, due to heterogeneity in PSMA expression, there is a high variation.

Overview immunofluorescent staining

In Table 6, a summary of the immunofluorescence staining is presented. The score is based on a subjective interpretation from an independent individual. The immunofluorescent images (without the name of the belonging cell line and condition) were shown to an individual, which ranked the images based on the intensity of the green and red staining in the cytoplasm of the cells in an unbiased manner.

Table 6: Summary of immunofluorescence PSA and PSMA staining in different PCa cell lines.

Disease state	Cell line	Passage number	PSA			PSMA		
			- R1881	+R1881	+Enzalutamide	- R1881	+R1881	+Enzalutamide
Be	PWR-E1	Px+12	-	-	++	-	-	-
	RWPE-1	76	-	-	-	-	-	-
HS	RWPE-2	77	+	++	-	-	-	-
	LNCaP	52	++	+++	+	++	+++	++
CR	22Rv1	Px+21	-	+	-	+	+	-
	PC-3	109	-	-	-	-	-	-

PSMA is expressed in PCa cells and it can be increased in mCRPC cells. In our study, PSMA expression was only detected in LNCaP (hormone-sensitive) and 22Rv1 (castration-resistant) cells. PSMA levels were higher in the hormone-sensitive LNCaP cells compared to the castration-resistant 22Rv1 cells. This is in line with the literature (Gorges et al., 2016)(Xia et al., 2021). In addition, an increase in PSMA expression was identified after androgen stimulation in LNCaP cells. The differences in PSMA expression in the different hormone-sensitive and castration-resistant cell lines can be due to heterogeneity of PSMA expression (Sheehan et al., 2022).

PSA expression was observed in PWR-E1 (benign), RWPE-2 (hormone-sensitive), LNCaP (hormone-sensitive) and 22Rv1 (castration-resistant) cells. Androgen stimulation (R1881) was expected to increase PSA levels and enzalutamide to decrease PSA levels in hormone-sensitive cells. This was also the case in the hormone-sensitive RWPE-2 and LNCaP cell lines.

Figures 9,10,12 and18 suggest nuclear localization of PSA. However, nuclear localization of PSA was also observed in the negative control HEPG2 cell line (Supplementary Figure 10) and in the PSA negative cell line PC-3 (Figure 18). This was not identified in the literature (Kuske et al., 2016). In addition, other studies detected cytoplasmic PSA instead of PSA throughout the nucleus (Theil, Bialek, Weiß, Lindner, & Fornara, 2022)(Tang, 2022)(Qin et al., 2012). Therefore, we identified nuclear PSA staining as non-specific, this could be attributed to the non-specific binding of the secondary antibody to the cell nucleus. To confirm this, the primary antibody in a next experiment should be absent.

3.3 Secretions study of prostate cancer cell lines in response to drugs

The prostate cancer cell lines were further evaluated for their PSA secretion in response to androgen stimulation and inhibition. This chapter will provide a comparative analysis of the PSA secretions in the supernatant and from single cells, among the different PCa cell lines in response to androgen stimulation and AR inhibition.

3.3.1 PSA detection in the supernatant (dot blot)

The supernatant of the cells was collected after 7 days from a flask of 60-80% confluency and spotted on a PVDF membrane. Using a staining protocol which is illustrated in Figure 19, the PSA in the supernatant is detected.

An example of how fluorescence spots of supernatant of LNCaP cells look on a membrane is shown in Figure 20.

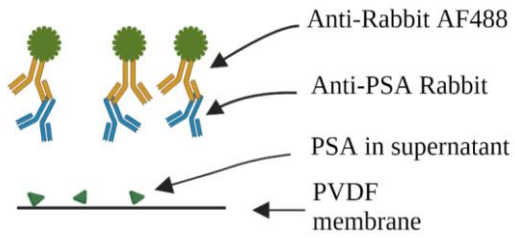

Figure 19: Illustration of the detection of PSA in the supernatant of PCa cell lines. Supernatant is spotted on a PVDF membrane. In the case of PSA in the supernatant, anti-PSA Rabbit bounds to the PSA. Using anti-Rabbit AF488 the PSA is visualised. Created with Biorender.com

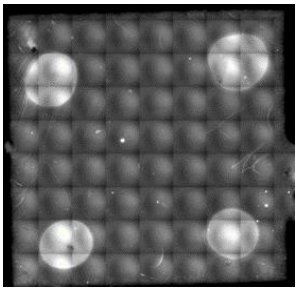

Figure 20: Four droplets of supernatant of LNCaP cells on a PDVF membrane.

The area and the mean intensity of the fluorescent spot can be determined using ImageJ. The mean intensity of the membrane is subtracted.

Using a calibration curve, the data can be converted into quantitative data and the exact amount of PSA can be determined. However, the calibration curve (Supplementary Figure 1) could not be optimized due to the lack of reproducibility. The current calibration curve resulted in unreliable exact amounts of PSA, compared with the ELISA experiment and literature. Therefore, it was decided not to use the calibration curve and to use relative values to compare PSA secretion between cell lines and conditions.

3.3.1.1 LNCaP (hormone-sensitive)

The supernatant of LNCaP cells was spotted (2 µL droplets) on a membrane as shown in Figure 21. The fluorescent spots indicated PSA secretion by LNCaP cells. It is well known that LNCaP cells secrete PSA (Sasaki et al., 2016) (Yamamoto et al., 2020)(Deep et al., 2008). The mean intensity of the fluorescence spots is 1129 units. Due to the lack of a calibration curve, it is not known how many ng PSA is in one spot.

The images of the membranes showed the presence of black lines (Figure 21) which can be attributed to a limitation of the camera. This resulted in an intensity difference in a single image. The left sight of a single image has a lower intensity compared to the rest of the image

(Supplementary Figure 11). Therefore, the fluorescent spots lack a homogeneous intensity thereby influencing the mean intensity.

No fluorescent dots were detected when spotting the cell culture medium of LNCaP cells on a membrane.

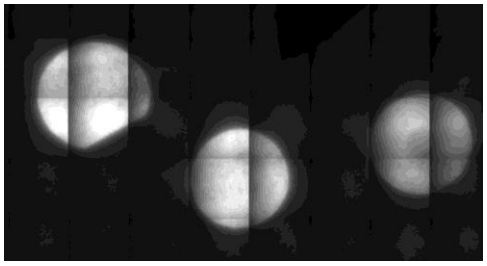

Figure 21: Three droplets of 2 µL of supernatant of LNCaP cells spotted on a PVDF membrane.

3.3.1.2. 22Rv1 (castration-resistant)

A membrane with spots of the supernatant of 22Rv1 cells is shown in Figure 22. The spots were a bit dimmer than the spots of the supernatant of LNCaP cells, as shown in Figure 21. This corresponds to the mean intensity of the spots, which is 90 units for the fluorescence spots of the 22Rv1 cells and 1129 units for the spots of LNCaP cells. This is consistent with similar observations in the literature. Other studies reported lower levels of PSA secretion by 22Rv1 cells compared to LNCaP cells. These results were acquired using western blot (Sasaki et al., 2016) (Deep et al., 2008).

No fluorescent dots were detected when spotting the cell culture medium of 22Rv1 cells on a membrane.

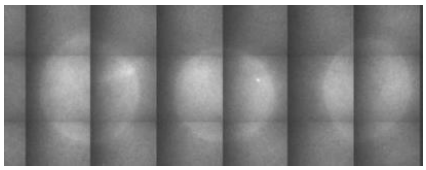

Figure 22: Three droplets of 2 µL of supernatant of 22Rv1 cells spotted on a PVDF membrane.

3.3.1.3 EMC-PCa-41(castration-resistant)

A membrane with spots of supernatant of EMC-PCa-41 organoid cells is shown in Figure 23. The supernatant was collected 48 hours after refreshing the cell culture medium and at different times (1st week, 2nd week and 6th week) after thawing of the EMC-PCa-41 organoid cells. The fluorescent spots were dim, a mean intensity of 32 (1st week), 34 (2nd week) and 21 (6th week) units is measured.

However, these data must be interpreted with caution because very dim dots were also observed after spotting the medium of EMC-PCa-41 cells (Supplementary Figure 12). This could be due to

some components in the APCOM medium. A mean intensity of 21 units of the dots of the APCOM was measured, which is comparable to the mean intensity of the supernatant which is collected in the 6th week after thawing.

The mean intensity value of the spots of the medium of EMC-PCa-41 cells was subtracted from the mean intensity from the supernatant from the EMC-PCa-41 cells.

No earlier research is done into PSA secretion of EMC-PCa-41 cells. However, L. Mout et all reported positive PSA IHC staining. In addition, positive KLK3 (PSA encoded gene) expression was identified by qRT-PCR (Mout et al., 2021).

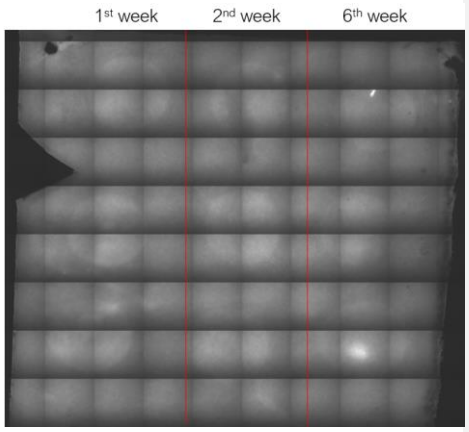

Figure 23: Nine droplets of 2 µL of supernatant of EMC-PCa-41 cells spotted on a PDVF membrane. Each row represents three droplets of supernatant of EMC-PCa-41 cells obtained from a different date.

3.3.1.4 Overview

No fluorescent spots of the spotted supernatant of the cell lines RWPE-1, RWPE-2, PWR-E1, PC-3 and HEPG2 were observed. This is in accordance with the literature. Other studies did not identify PSA in the supernatant of these cell lines using western blot (Sasaki et al., 2016) (Yamamoto et al., 2020)(Deep et al., 2008)(Tai et al., 2011).

In the hormone-sensitive cell line LNCaP higher PSA levels were detected in the supernatant compared to the PSA levels in the castration-resistant cell lines. No PSA secretion was detected in the supernatant from the benign cell lines. An overview of the findings is presented in Table 7.

Table 7: Overview: PSA observed in supernatant in the PCa cell lines.

Disease state	Cell line	Mean intensity of fluorescent spot in units	Passage numbers
Be	PWR-E1	Below detection limit	Px+13
	RWPE-1	Below detection limit	77
HS	RWPE-2	Below detection limit	81
	LNCaP	1129	53
CS	22Rv1	90	Px+26
	PC-3	Below detection limit	112
Organoids	EMC-PCa-41 (1st week) EMC-PCa-41 (2nd week) EMC-PCa-41 (6th week)	11 13 Below detection limit	Px+1 Px+1 Px+2

3.3.2 PSA detection on membranes.

To evaluate the PSA secretion from the single cells, cells were seeded on an anti-PSA coated membrane for 24 and 48 hours. The cells are seeded on a membrane in three different conditions (untreated, androgen stimulated, AR inhibited) as mentioned in Section 2.5. Using a staining protocol (Figure 24) the captured PSA on the PVDF membrane can be visualized.

An example of how a membrane with captured PSA looks, is shown in Figure 25.

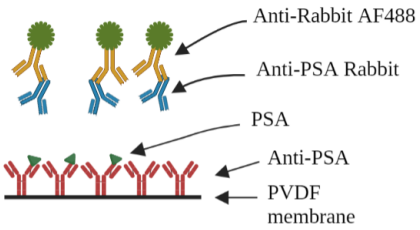

Figure 24: Illustration of detection of captured PSA on coated PDVF membranes. PVDF membrane is coated with anti-PSA. PSA secreted by cell lines is captured on the coated membrane. An anti-PSA rabbit AB and anti-rabbit AF488 AB are added to visualize the captured PSA. Created with Biorender.com

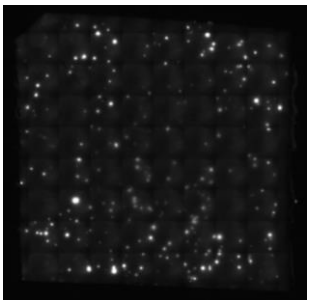

Figure 25: PVDF membrane with captured PSA, secreted by 2000 LNCaP cells.

3.3.2.1 Quantification

The images were further analysed with ImageJ to identify PSA secretion spots and quantitatively assess PSA secretion in response to drugs.

Montages of the membranes were opened in ImageJ and a duplicated image is created. The duplicated image was saved as a 10-bit image and an intensity threshold of 550 was set. This threshold was chosen based on membranes of LNCaP and HEPG2 cells. On the membranes of the LNCaP cells, it was observed that at this threshold most of the spots are not merged, see Figure 26. In addition, not many spots are missed. On the membranes of the HEPG2 cells, only a few small spots were detected at this threshold. A binary image was created in which pixels with an intensity higher than 550 units become black and pixels with an intensity lower than 550 units become white, as shown in Figure 27. The black dots were the regions of interest. The binary image was linked to the original image. From the pixels

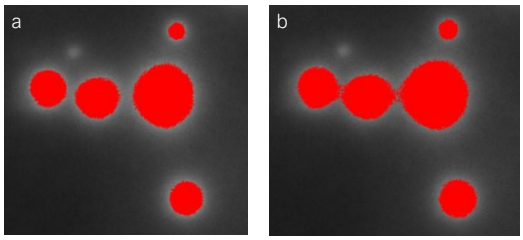

Figure 26: PVDF membranes with PSA secretion of LNCaP cells. Red indicates an intensity above the intensity threshold. a) Intensity threshold set at 550. Spots are not merged. B) Intensity threshold set at 500. Three spots are merged.

of the black dots in the binary image, the area and the mean intensity in the original image were computed. The intensity values were normalized to the background and HEPG2 cells.

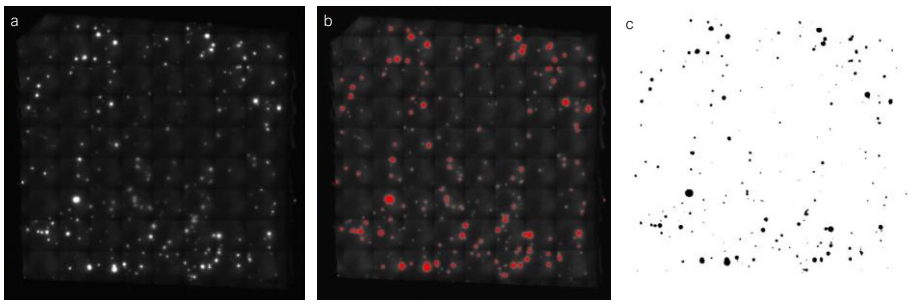

Figure 27: a) PDVF membrane with PSA secretion spots of untreated LNCaP cells. b) An intensity threshold is set at 550. Red pixels indicate an intensity above 550. C) Binary image created with the intensity threshold of 550. Red pixels become black, the other pixels become white.

The area of the dot was multiplied by the mean intensity of the dot. This gives a value of the amount of PSA that is secreted by the cell which is correlated to the dot, see Figure 28. A more elaborated quantification protocol is present in the Supplementary Data.

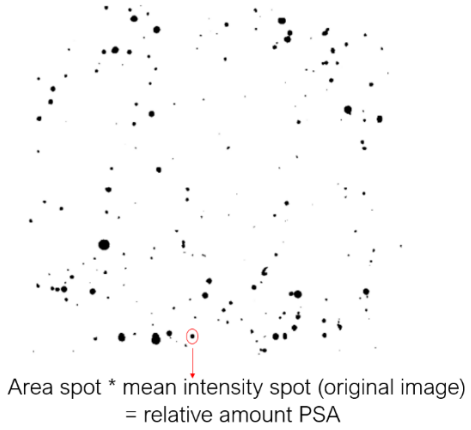

Figure 28: An illustration to calculate the relative amount PSA which is secreted by an individual cell. Black dots are the regions of interest. The area of a dot is multiplied by the mean intensity of the pixels of the original image, located at place of the black dot.

Due to a change in microscopic fiber during the experiments, there is a change in exposure time and in the intensity threshold between some datasets. An overview of the datasets and their properties is shown in Supplementary Table 1. Due to the lack of a calibration curve, which is scanned with both fibers, it is not possible to compare the datasets which are scanned with a different fiber.

3.3.2.1 Negative controls

As a negative control, HEPG2 cells were used and treated as per protocols mentioned in Section 2.5.2. HEPG2 origins from human hepatocyte carcinoma (Donato, Tolosa, & Gómez-Lechón, 2015) and do not secrete any PSA. As an extra negative control, an empty membrane was treated the same as the other cell lines. The empty membranes looked similar to membranes on which HEPG2 cells were seeded. Small dim dots were visible on both membranes, as shown in Figures 29 and 30. These spots are probably not PSA secretion. The detected spots could be artefacts, clustering of staining antibodies or background spots of the membrane.

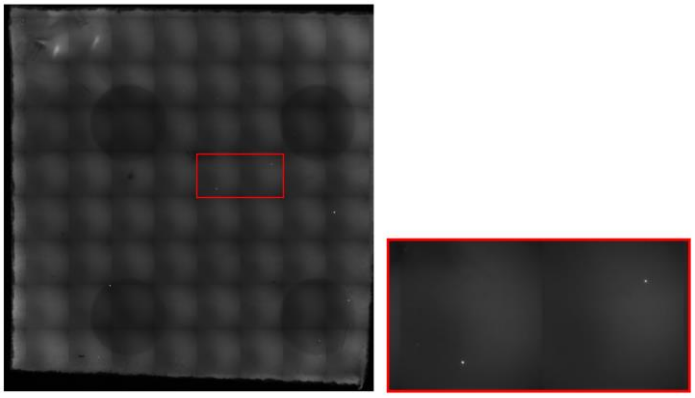

Figure 29: Empty PVDF membrane which are treated according to the protocols listed in Section 2.5.2, stimulated with R1881. Small fluorescence dots are detected.

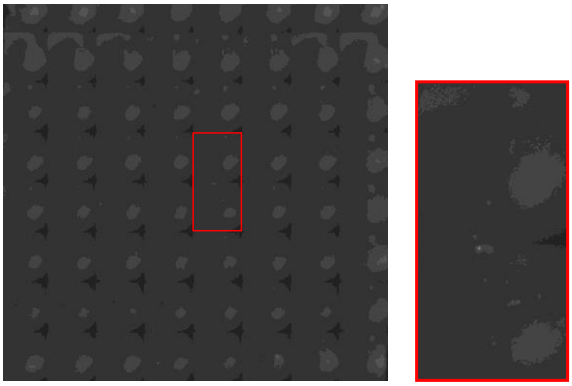

Figure 30: Membrane seeded with HEPG2 cells which are stimulated with R1881. Small fluorescence dots are detected.

The quantification method was applied to all these membranes. The results are shown in Figure 31.

The mean value of all PSA spots of HEPG2 cells ($1.3*10^6$ for experiments with old fiber and $5.3*10^6$ for experiments with new fiber) was in the same range as the mean value of the PSA spots detected from the empty membrane ($3.7*10^6$)

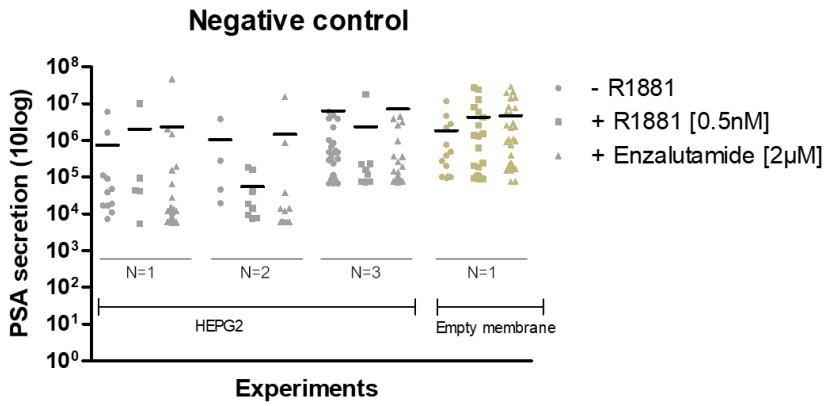

Figure 31: Detected spots of seeded HEPG2 cells and empty membranes after 24 hour. For HEPG N=3, for empty membrane N=1. Students t-test was performed to confirm significance.

The mean value of all spots of the HEPG2 cells is used as a threshold for the other cell lines in the next experiments. All spots with a value of less than the mean value of HEPG2 cells are considered not to be secretion and are not shown in the following graphs (HEPG2 passage numbers unknown).

3.3.2.2 LNCaP (hormone-sensitive)

The membranes with PSA secretion of LNCaP cells of one experiment are shown in Figure 32.

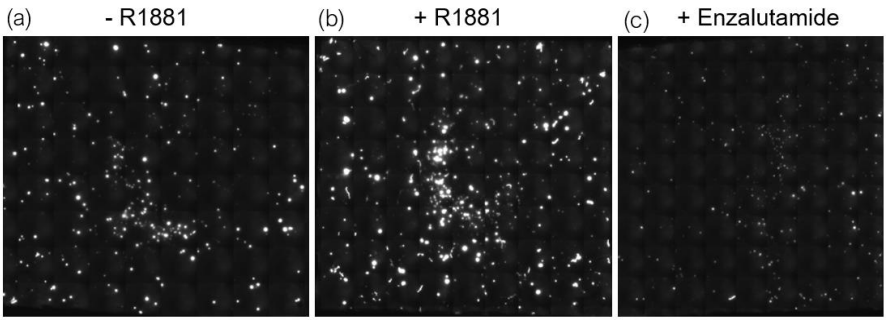

Figure 32: Membranes with captured PSA from LNCaP cells under different conditions after 24 hour. Upon androgen stimulation with R1881 more and bigger PSA spots are identified. After treatment with Enzalutamide smaller dimmer PSA spots are identified. A) Captured PSA of 2000 untreated LNCaP cells. b) Captured PSA of 2000 cells LNCaP cells which are stimulated with R1881 [0.5nM] for 24 hour. C) Captured PSA of 2000 LNCaP cells after 24 hour treatment with Enzalutamide [2 μM]. Before the 24 hour Enzalutamide treatment, the LNCaP cells were overnight stimulated with R1881 [0.5 nM]. Passage number = 41.

An anti-PSA coated PDVF membrane can capture PSA which is secreted by LNCaP cells, as shown in Figure 32. When the LNCaP cells were stimulated with R1881, most of the PSA secretion spots become bigger. When the cells were AR inhibited using Enzalutamide the PSA secretion spots become smaller.

Single cell PSA secretion

The values for PSA (mean intensity spot * area spot) secreted by individual LNCaP cells after 24 and 48 hours are shown in a scatterplot in Figure 33. The repeated experiments are shown in the graph. The assumption is that each spot on the membrane belongs to a single cell. It is not possible to confirm this, because there is no image of the cells on the membrane, with which to correlate the spots.

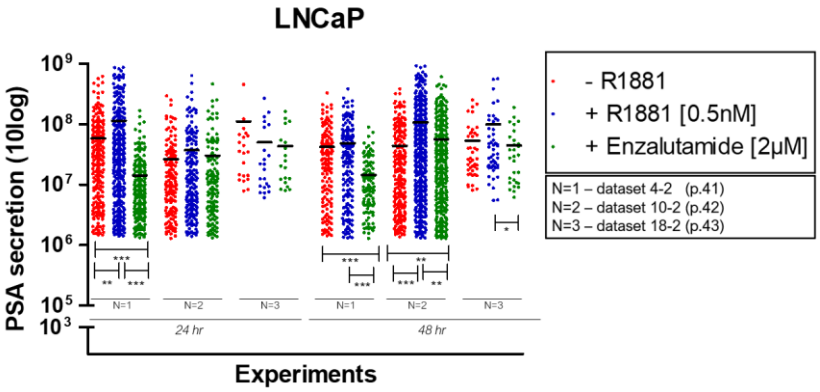

*Figure 33: Detected PSA secretion of single LNCaP cells after 24hour and 48hour under different conditions. The black line represents the mean. In general higher PSA values are observed after androgen stimulation (R1881), and lower PSA values are observed after treatment with Enzalutamide. Data was normalized to the HEPG2 cell line. Students t-test was performed to confirm significance. * 0.05 < P; **0.01< P; ***0.001< P*

Wide variation in PSA secretion

There is a wide variation in the amount of PSA that each cell secretes as shown in Figure 33. This corresponds to the images of the membranes (Figure 27). Both small dim dots and bigger brighter dots were visible on the membrane, indicating a high variation in PSA secretion per cell. This can be due to heterogeneity, some cells secrete more PSA than others. Other studies showed also heterogeneity in PSA secretion from LNCaP cells (Abali et al., 2021). In addition, it is not sure if each spot is derived from a single cell. It can be that multiple cells were clustered and their secreted PSA is at the same location on the membrane.

It should also be noted that despite the well-considered choice of the intensity threshold, some spots were merged. This resulted in one spot with a larger area instead of multiple smaller spots. This may result in higher values.

Influence of androgen activation and inhibition

The results indicated that androgen stimulation leads to an increase in PSA secretion compared to the untreated cells (one exception: third experiment, 24 hour timepoint), as seen in Figure 33. After treatment with enzalutamide, a decrease in PSA secretion was observed, compared to the androgen stimulated cells. In most experiments, the amount of PSA secreted after treatment with enzalutamide, was also lower compared to the untreated cells (two exceptions, second experiment (N=2), both after 24 and 48 hours).

The exceptions can be attributed to multiple factors such as the passage number, the confluency or the different cell cycle stages of the cells. Heterogeneity can also be a reason for the variation in trends. It can be that not all cells are affected by Enzalutamide or require a higher drug concentration.

The increase in PSA secretion after androgen stimulation and decrease in PSA secretion after treatment with anti-androgens is in line with what is found in the literature. C.S. Mathy et al. reported that the anti-androgen abiraterone induces a concentration-dependent decrease in PSA secretion (Mathy et al., 2021). In addition, F. Abali et all. showed increased PSA secretion upon androgen stimulation and decreased PSA secretion when LNCaP cells were treated with the anti-androgens enzalutamide and abiraterone (Abali et al., 2021).

24 hour versus 48 hour

It was expected that more PSA secretion was detected after 48 hours compared to 24 hours because cells have more time to produce and secrete PSA. However, no differences in trends of PSA secretion were observed between the timepoints 24 and 48 hours (Figure 22). It could be that the cells require more stimulation over time, or that the cells reach saturation of PSA secretion. Another possible explanation is that there was a difference in PSA secretion between the timepoints, but that this technique is not sensitive enough to visualize it on the membranes.

Percentages of PSA secreting cells

2000 cells were seeded on the membrane but not more than 400 spots were detected on the membranes. This indicates that not all cells secrete PSA. Approximately 7% of the untreated cells secrete PSA. The study of F. Abali et all. showed that 53% of viable LNCaP cells secrete PSA (Abali et al., 2021). However, the method differs in several important ways. In the study of F. Abali the exact amount of live LNCaP cells was known. In our research is the exact amount of living LNCaP cells not known. In addition, it is not known if a secretion spot belongs to one or multiple cells.

The percentages of PSA secreting cells are presented in Figure 34.

After 24 hours, it was observed that with stimulation, the number of PSA secreting LNCaP cells was increased by 2.2 %. While after AR inhibition, a small decrease of PSA secreting LNCaP cells (0.4%) was observed (Figure 34). After 48 hours, there was also an increase in PSA secreting cells after androgen stimulation (2.7%), however, no decrease in the number of PSA secreting cells was seen after treatment with Enzalutamide compared to the untreated cells. The AR inhibited condition did show a decrease in PSA secreting cells compared to the androgen stimulated condition (1.8%).

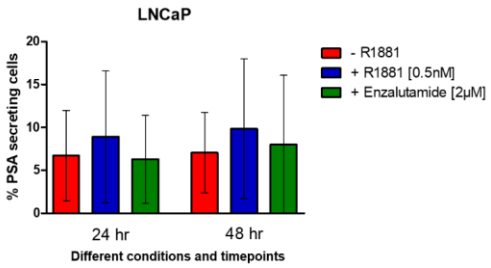

Figure 34: Percentages of PSA secreting LNCaP cells after 24 and 48 hour upon androgen stimulation and inhibition. Data represents mean ± sd (n=3). Students t-test was performed to confirm significance. Passage numbers of LNCaP cells were 41, 42 and 43.

Summarized, the results indicate that a higher number of LNCaP cells secrete PSA after androgen stimulation. However, these results have a high standard error and are not significant. This can be attributed to the fact that fewer secretion spots were detected for the experiment repeated for the third time (N=3). However, the cells were treated the same as in the previous experiments and showed healthy morphology.

There are some drawbacks to our method which result that the percentages of PSA secreting LNCaP cells are not fully reliable. First of all, it can be that cells are clustered together, which results in one big PSA secretion spot on the membrane instead of multiple smaller spots. This reduces the number of detected PSA spots. In addition, there is mentioned that 2000 cells were seeded on the membrane. However, this is with a large error. This is because the cells were counted with the luna counter, which is not the most reliable method to count cells. In addition, only 2000 cells were needed from a cell suspension of approximately 2,5 million cells. This means that only a really small volume was needed from a bigger volume. It is a rough estimation that 2000 cells are in the small volume that is taken. In addition, the cell suspension was added to a square membrane in a round well plate. As a result, cells were also able to attach to the bottom of the well plate next to the membrane instead of on the membrane.

However, the method was consistently used for analysing every membrane and hence, is comparable for all cell lines of different time points and conditions.

Total PSA secretion

Next, the total amount of PSA that is secreted by 2000 LNCaP cells was calculated by adding the PSA values of all individual cells. This data is presented in Figure 35. The graph implicates that the androgen stimulated cells secreted in total a higher amount of PSA, while in comparison, the inhibited cells secreted in total less PSA.

In addition, it was observed that the decrease in PSA secretion of inhibited cells was more in 24 hours than in 48 hours. A possible explanation is the loss of the inhibitory function of the drug after 24 hours.

The trend of increase in PSA secretion after androgen stimulation and decrease in PSA secretion after treatment with anti-androgens is in accordance with the literature (Mathy et al., 2021)(Abali et al., 2021)

LNCaP is a hormone-sensitive cell line. PSA secretion of LNCaP cells is affected by the anti-androgen enzalutamide. Enzalutamide is also used for the treatment of mHSPC patients. These results suggest that LNCaP cells can be used as a good model for mimicking the PSA secretion response to anti-androgens in mHSPC patients.

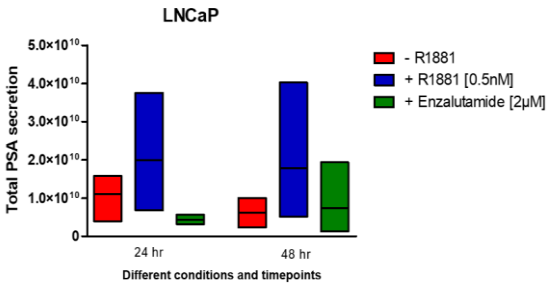

Figure 35: Total amount of PSA secreted by LNCaP cells upon androgen activation and inhibition after 24 and 48 hour. Data represents min to max with mean (n=3.) Passage numbers of LNCaP cells were 41, 42 and 43.

3.3.2.3 Other prostate cancer cell lines

PSA secretion

The detected PSA spots, secreted by single cells of different PCa cell lines, are presented in Figure 36 (N=3). Only a few spots were detected in each cell line. In addition, there was not a clear trend between the conditions (untreated, androgen stimulated and AR inhibited) and also between the different cell lines. Graphs with more details of the individual cell line are presented in the Supplementary Data (Supplementary Figures 15-19).

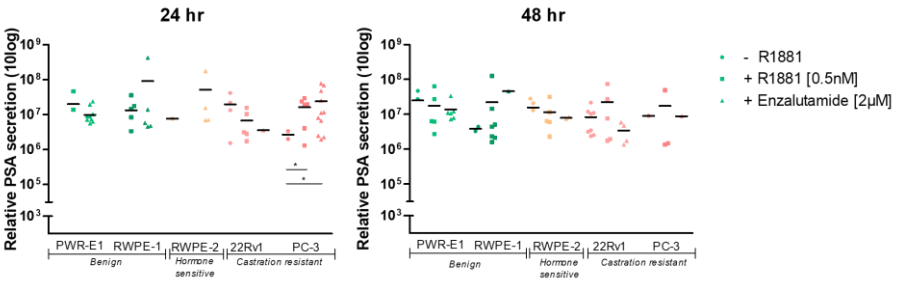

*Figure 36: Detected PSA secretion of single PCa cells after 24 and 48 hour under different conditions. The black line represents the mean. No clear trend was observed. Data was normalized to the HEPG2 cell line. Students t-test was performed to confirm significance. * 0.05 < P; **0.01< P; ***0.001< P (N=3, data is combined)*

The main limitation of this method, to detect PSA secretion from single cells on membranes, is that it is not possible to distinguish between PSA secretion and unspecific binding or artifacts on the membrane. From PC-3 cells is well known that they do not secrete PSA. However, some PSA spots were detected on the membranes of PC-3 cells. This is probably not PSA secretion. From 22Rv1 is known that it secretes PSA, this was also detected in the supernatant. However, the number of detected spots and the PSA value of these spots on the membrane of 22Rv1 cells, were comparable to the detected spots on the membrane of the PC-3 cell line. It is difficult to determine if the spots, developed by 22Rv1 and the other cell lines, are true PSA secretions.

A microwell chip should be used to overcome this problem and to be able to conclude what is a PSA secretion spot and what is not. Using this chip, the secretion spots on the membrane can be correlated with the cells in the chip. To confirm if a spot is protein secretion, the corresponding well with the cell can be evaluated. The presence of a cell in the microwell can confirm the possibility of secretion otherwise, it can be regarded as unspecific staining or artifacts on the membranes.

In addition, spots on the membrane were missed due to a too low intensity value. Using the microwell chip it can be determined if these spots are protein secretion. If these spots are protein secretions, adjustments in the quantification protocol must be made to include these spots.

PSA secretion versus intracellular PSA

Intracellular PSA was observed in LNCaP cells, androgen stimulated RWPE-2 cells and in a low amount in 22Rv1 cells. It is difficult to identify if the intracellular PSA is in line with the PSA secretion of the cell lines RWPE-2 and 22RV1, as this method (Section 2.5.2) fails to distinguish between PSA secretion and artefacts.

Percentages of PSA secreting cells

The percentages of PSA secreting cells after 24 hours and 48 hours are shown in Figure 37. The percentages of PSA secreting cells were very low. There was no trend between the different conditions. In addition, there was no significant difference within different conditions. The percentages of PSA secreting cells of the PCa cell lines are comparable to the negative control cell line HEPG2. There is need for a reliable method which can distinguish between PSA secretion and artifacts.

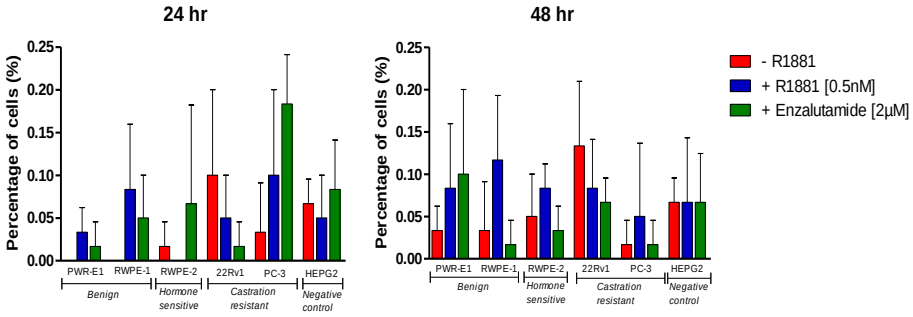

Figure 37: Percentages of PSA secreting cells after 24 and 48 hour upon androgen stimulation and inhibition. No clear trend was observed. Data represents mean ± sd (n=3).

Overview

An overview of the PSA secretion for each cell line is presented in Table 8.

Table 8: Overview: PSA secretion by different PCa cell lines.

Disease state	Cell line	Relative mean PSA per cell			% secreting cells		
		-R1881	+R1881	+ Enzalutamide	-R1881	+R1881	+ Enzalutamide
Benign	PWR-E1 24hr	0	$2*10^7$	$0.4*10^7$	0%	0.03%	0.1%
	48hr	$2.5*10^7$	$1.8*10^7$	$1.4*10^7$	0.03%	0.01%	0.02%
	RWPE-1 24 hr	0	$1.3*10^7$	$9.1*10^7$	0%	0.08%	0.05%
	48hr	$0.4*10^7$	$2.2*10^7$	$4.7*10^7$	0.03%	0.1%	0.02%
HS	RWPE-2 24hr	$0.8*10^7$	0	$5.2*10^7$	0.02%	0%	0.07%
	48hr	$1.6*10^7$	$1.1*10^7$	$0.8*10^7$	0.05%	0.08%	0.03%
	LNCaP 24hr	$6.5*10^7$	$6.7*10^7$	$2.9*10^7$	6.7%	8.9%	6.3%
	48hr	$4.6*10^7$	$8.5*10^7$	$3.9*10^7$	7.1%	9.8%	8%
CS	22Rv1 24hr	$2*10^7$	$0.7*10^7$	$0.4*10^7$	0.1%	0.05%	0.02%
	48hr	$0.8*10^7$	$2.2*10^7$	$0.3*10^7$	0.1%	0.07%	0.07%
	PC-3 24hr	$0.3*10^7$	$1.6*10^7$	$2.4*10^7$	0.03%	0.1%	0.2%
	48hr	$0.9*10^7$	$1.7*10^7$	$0.9*10^7$	0.02%	0.05%	0.02%

The advantage of this method, using a PVDF membrane, is that PSA secretions from single cells can be detected and quantified. Apart from PSA, other proteins of interest can also be analysed to assess the effect of drugs on different cell lines. However, the seeded cells can not be directly

correlated to their secretions. Using a microwell chip, secretion spots can be correlated to the cells located in each microwell. This is a potential platform to perform single cell proteomic analysis, isolate cells of interest and perform further downstream analysis to look into the possible phenotypic and genotypic heterogeneity within treated cells.

3.3.3 Enzyme-linked immunosorbent assay

Enzyme-linked immunosorbent assay (ELISA) was performed to quantify the secreted PSA by the different PCa cell lines. In Figure 38 the amount of PSA secreted by different PCa cell lines after 7 days of culturing in the T25 flask is shown. Three supernatant samples of the EMC-PCa-41 organoid cell line are presented. These samples were stored one week, two weeks and six weeks after thawing the organoid cell line.

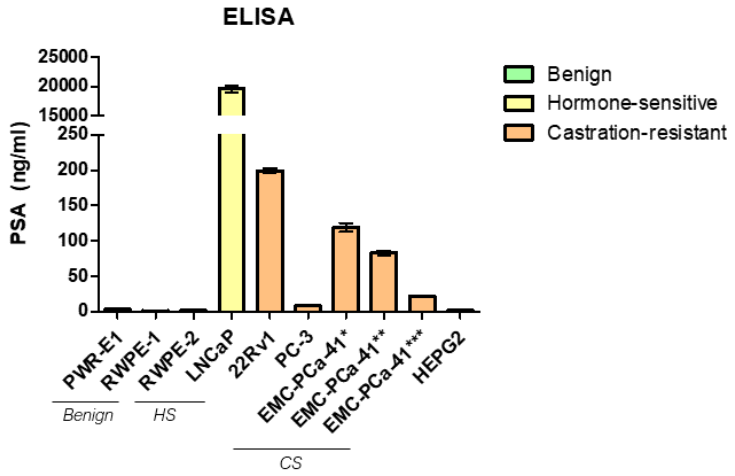

*Figure 38: PSA in the supernatant of different PCa cell lines. The supernatant is stored after seven days. PSA is detected in supernatant of LNCaP, 22Rv1 and EMC-PCa-41 cells. *One week after thawing ** Two weeks after thawing ***Six weeks after thawing*

Hormone-sensitive cell line LNCaP showed the highest PSA secretion levels (19600 ng/ml). In addition, PSA secretion of castration-resistant 22Rv1 cell line (200 ng/ml) and the castration-resistant organoid cell line EMC-PCA-41(119 ng/ml, 83 ng/ml, 22 ng/ml) was detected.

Remarkably, the PSA secreted by EMC-PCa-41 cells decreases with time. This could be due to fewer healthy living cells in the wells plate after the repetitive medium change, which can bring down the PSA production. Four weeks after thawing, the organoid cells were passaged. This could also result in loss of cells and so less cells which can secrete PSA.

These findings are in line with the results of spotting supernatant on the membrane. The highest PSA concentration was found in the supernatant of LNCaP cells and a lower amount of PSA in the supernatant of 22Rv1 and EMC-PCa-41 cells.

F. Abali et al. detected around 5 pg PSA per LNCaP cell per day (Abali et al., 2021). This is in line with the findings of our study. Assuming 500.000 cells per ml, around 5.6 pg PSA per LNCaP cell per day was expected in our study(19.600ng/ml /7 days /500.000 cells *1000).

Literature showed also contradictory findings. S. Bhamre et al., detected 252 ng PSA per $1*10^6$ LNCaP cells after 24 hours (Bhamre, Whitin, & Cohen, 2003). Assuming 500.000 cells per ml, around 5600 ng PSA per $1*10^6$ LNCaP cells after 24 hours was expected in our study.

In addition, T. Yamamoto et al. detected around 6 ng PSA per ml after 48 hours of culturing (Yamamoto et al., 2020) using ELISA. However, T. Yamamoto et al. did not mention the number of cells, which makes it hard to compare the data. These findings have lower PSA secretion levels than our findings.

These contradictory results may be due to some limitations of this experiment. The ELISA was only performed once. The experiments must be repeated to confirm the findings. In addition, there was no optimized protocol for the ELISA with our cell lines and PSA as proteins of interest. Based on other studies, the concentrations for a calibration curve and dilution factors for supernatant of the cell lines were chosen. However, the PSA concentrations in the LNCaP, 22Rv1 and EMC-PCa,41 cell supernatants did not fell within the linear portion of the standard curve (0–60 ng PSA). For a next experiment, other dilution factors are recommended, which are presented in Table 9. When the PSA concentrations from all cell lines fall within the linear portion of the standard curve, the quantitative results will be more reliable.

Table 9: Recommended dilution factors for samples ELISA

Cell line	Condition	Dilution factor
LNCaP	Supernatant collected after 7 days. On day 7 a 80% confluency. T25 flask.	500x
LNCaP	100.000 cells seeded in 24-wells plate Supernatant collected after 48hour.	500x
LNCaP	100.000 cells seeded in 24-wells plate. Stimulated with R1881. Supernatant collected after 48hour.	800x
22Rv1	Supernatant collected after 7 days. On day 7 a 80% confluency. T25 flask.	5x
22Rv1	100.000 cells seeded in 24-wells plate. Supernatant collected after 48hour.	5x
22Rv1	100.000 cells seeded in 24-wells plate. Stimulated with R1881. Supernatant collected after 48hour.	5x
EMC-PCa-41	Cells seeded in Matrigel. Supernatant collected after 48 hours.	2x

Remarkable is that a low amount of PSA was observed in the PC-3 cell line. From PC-3 cells is known that they do not secrete PSA (Tai et al., 2011)(Yamamoto et al., 2020) and in our dot blot assay also no PSA was detected in supernatant of PC-3 cells. In addition, in another ELISA experiment, no PSA was detected in the supernatant of PC-3 cells (Figure 39). The detected PSA in this experiment (Figure 38) is probably due to artefacts.

No PSA was detected in the supernatant of the other cell lines. This corresponds to the results of the dot blot assay.

Influence of androgen stimulation on PSA secretion

In another experiment, 100.000 cells were seeded in a 24-wells plate. Half of the cells were untreated and the other half were androgen stimulated using R1881. The supernatant was stored after 48 hours and an ELISA was performed. The results are shown in Figure 39.

The untreated LNCaP cell secreted around 6787 ng PSA per 100.000 cells per 48 hours (33 pg PSA per cell per day) and the androgen stimulated LNCaP cells secreted around 17885 ng PSA per 100.000 cells per 48 hours (90 pg PSA per cell per day). Androgen stimulation had a significant increasing influence on the PSA secretion of the hormone-sensitive LNCaP cell line. In

the results of Section 3.3.2.2 also an increase in PSA secretion by LNCaP cells after androgen stimulation was detected. Unfortunately, we don't have exact values of these experiments. Therefore we can not compare the amount of PSA secreted with the single cell membrane experiment.

Untreated 22Rv1 cells secreted around 75 ng PSA per 100.000 cells per 48 hours (0.37 pg PSA per cell per day). When the cells were androgen stimulated around 84 ng PSA per 100.000 cells per 48 hours (0.42 pg PSA per cell per day) is detected. This is a small increase, but not a significant difference. From the single 22Rv1 cells on a PVDF membrane (Section 3.3.2.3) was a negligible amount of PSA secretion detected and even no influence of R1881.

ELISA must be repeated with the previously described adjustments and the influence of the anti-androgen Enzalutamide should be included.

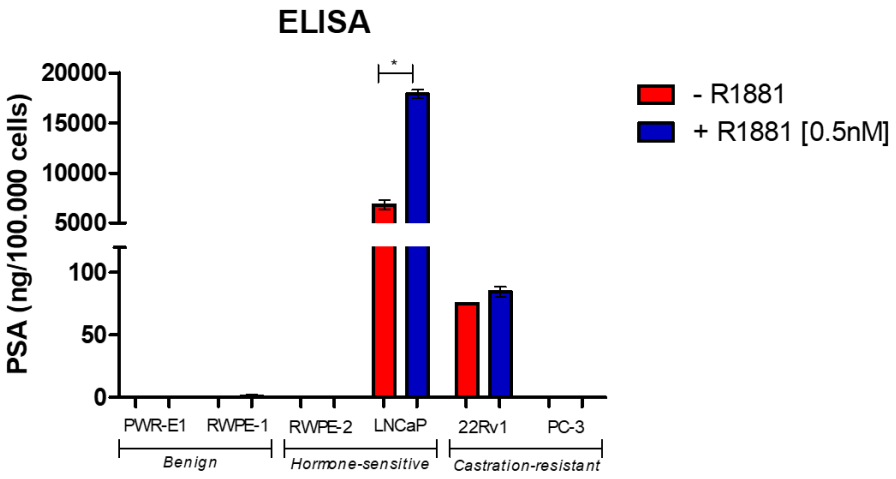

Figure 39: Effects of R1881 on PSA secretion in different PCa cell lines. The data indicate a significant increasing effect in PSA secretion upon stimulation with R1881 for LNCaP cells. For 22Rv1 cells no significant difference in PSA production is observed.

3.4 Expression study of prostate cancer cell lines

Using flow cytometry the expression of PSMA, HER2 and EpCAM was evaluated in different PCa lines and shown in Figure 40.

PSMA

The hormone-sensitive cell line LNCaP showed the highest expression for PSMA, as seen in Figure 40a. It is seen that the castration-resistant 22Rv1 cell line also expresses PSMA, but in a lower amount compared to LNCaP cells. This is in line with the results of the immunofluorescence staining, as described in Section 3.1.
In literature is stated that around 20-30% of 22Rv1 cells express PSMA and almost 100% of LNCaP cells express PSMA (Sheehan et al., 2022)(Staniszewska et al., 2021). This result in different levels of PSMA expression (low versus high), which is in accordance with our findings.

However, it is known that PSMA is highly expressed in PCa and can be increased in castration-resistant patients. Our results suggest higher PSMA expression for the hormone-sensitive cell line LNCaP, compared to the castration-resistant cell lines. This is probably due to the heterogeneity of PSMA expression (Sheehan et al., 2022). In addition, some PCa cell lines and patients lack PSMA expression, even castration-resistant cell lines.

This experiment did not identified PSMA expression for the castration-resistant PC-3 cell line, the hormone-sensitive RWPE-2 cell line and the benign PWR-E1 and RWPE-1 cell lines. This is in accordance with the results of the immunofluorescence staining, as described in Section 3.1.

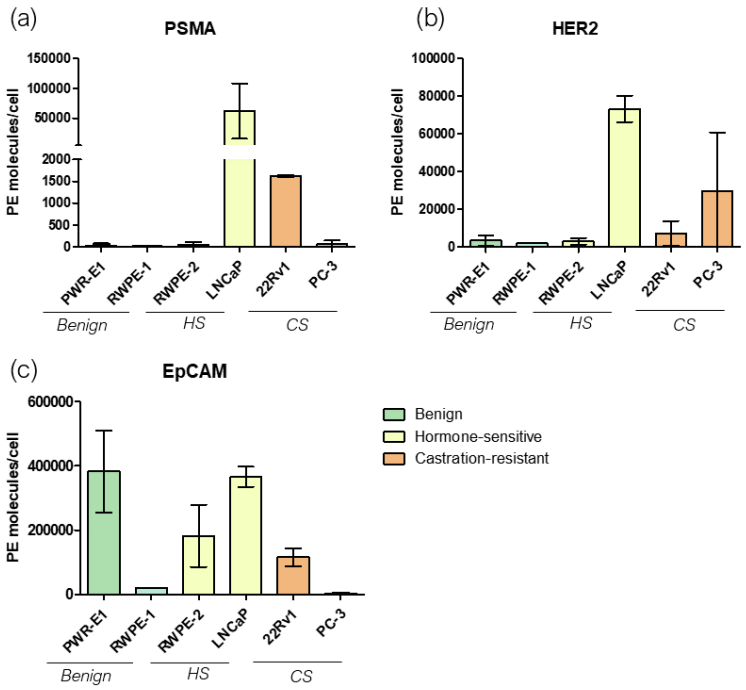

Figure 40: PSMA, HER2 and EpCAM expression in different PCa cell lines. A) PSMA expression is observed by LNCaP and 22Rv1 cells. B) Her 2 expression is observed by LNCaP, 22Rv1 and PC-3 cells. c) EpCAM expression is observed by PWR-E1, RWPE-2, LNCaP and 22Rv1 cells. Data represents the mean ± sd (n=2, exception for RWPE-1: n=1).

HER2

Hormone-sensitive cell line LNCaP showed the highest HER2 expression, as seen in Figure 40b, compared to the castration-resistant and benign cell lines. The castration-resistant cell line PC-3 showed also high HER2 expression, but there is a high variation between the different experiments. HER 2 expression is also detected in LNCaP and PC-3 cells in other studies (Malmberg, Tolmachev, & Orlova, 2011). In the other PCa cell lines low HER 2 expression was observed compared to LNCaP and PC-3 cells.

In HER2 positive breast cancer patients, HER2 targeted therapy is already proven to be an effective treatment (Dent et al., 2013). Studies reported also overexpression of HER2 in PCa (Day et al., 2017) (Sharifi et al., 2016). Investigating HER2 expression in different PCa cell lines, with various aggressiveness, and their response to different treatments can be used for exploring the possibility of using HER 2 as a biomarker for PCa.

EpCAM

In all PCa cell lines EpCAM expression was identified, but at different levels, as shown in Figure 40c. There is not a clear trend between benign, hormone-sensitive and castration-resistant cell lines. P. Massoner et al. observed EpCAM protein overexpression in PCa cell lines (LNCaP, PC-3) compared to benign cell lines (RWPE-1) (Massoner et al., 2014). In other studies also EpCAM expression is detected in the PC-3 cell line (Czaplicka et al., 2020)(Xu, Zhao, & Hou, 2014). This is partly contradictory to our findings. We did identified EpCAM overexpression in the LNCaP cell line compared to RWPE-1, but we did not identify overexpression in the PC-3 cell line. The experiment must be repeated to confirm these contradictory findings. In addition, the high EpCAM expression in the benign PWR-E1 cell line is remarkable. However, no earlier research on EpCAM expression in PWR-E1 cells is performed.

More data is required to establish EpCAM as prognostic biomarker or a potential EpCAM targeted therapy for PCa.

3.5 Overview data

In this section, the results of this research are summarized in Table 10.

Table 10: An overview of the results of all PCa cell lines.

Cell line		PWR-E1	RWPE-1	RWPE-2	LNCaP	22Rv1	PC-3	EMC-PCa-41
Single cell PSA secretion		No	No	No	Yes	No	No	-
% PSA secreting cells		0 - 0.25%	0 - 0.25%	0 - 0.25%	7.9%	0 - 0.25%	0 - 0.25%	-
PSA in supernatant	Membrane	No	No	No	Yes	Yes	No	Yes
	ELISA	No	No	No	Yes, ~19.600 ng/ml	Yes, ~200 ng/ml	No	Yes, ~120 ng/ml
Cellular PSA		Yes, upon AR inhibition	No	Yes, upon R1881	Yes	No to low levels	No	-
PSMA	Cellular	No	No	No	Yes	No to low levels	No	-
	Expression *(PE molecules/ Cell)*	27	18	45	62.252	1.627	63	-
EpCAM - Expression *(PE molecules/cell)*		382.581	21.396	182.297	366.344	115.545	3471	-
HER2 - Expression *(PE molecules/cell)*		3.321	2.045	2.973	73.149	7.137	29.666	-

4. Conclusion

In this study, we aimed to develop a realistic model to study the phenotypic response of PCa cell lines towards stimulation and inhibition of the AR, to obtain more insight into different PCa cell lines. Different PCa cell lines were characterized based on intracellular PSA, PSA secretion and expression of PSMA, EPCAM and HER2.

We detected PSA secretion from different malignant PCa cell lines (LNCaP, 22Rv1, EMC-PCa-41) and observed absence of PSA secretion in the benign cell lines. The hormone-sensitive cell line LNCaP showed higher levels of PSA secretion compared to the castration-resistant cell lines. In addition, we identified an increase in PSA secretion upon androgen stimulation and a decrease in PSA secretion after treatment with the anti-androgen enzalutamide, in LNCaP cells. These results suggest that LNCaP cells can be used as a model mimicking the responses to anti-androgens in mHSPC patients.

In addition, we discovered that detecting single-cell PSA secretion from low producing cell lines, using a PVDF membrane, (method in Section 2.5) is difficult. A low amount of PSA secretion is hard to distinguish from unspecific staining. The use of PVDF membranes to capture secreted proteins show promise, however, this method must be improved to study the phenotypic response of single cells.

Our findings indicate the presence of PSA secretion and PSMA, EpCAM, and HER2 expression in malignant PCa cell lines and the absence of PSA secretion and PSMA expression in benign cell lines. The hormone-sensitive cell line LNCaP shows higher levels of PSMA and HER2 expression compared to the benign and the castration-resistant cell lines.

Taken together, LNCaP cells can serve as a good model to study PSA secretion in response to drugs, with the use of a PVDF membrane. In the future, a microwell chip can help to identify the effect of drugs and stimulation on PSA secretion from the other PCa cell lines.

5. Future recommendations

In this chapter different limitations of our research and recommendations for future research are discussed.

We optimised a model to study the phenotypic response of single cells of PCa cell lines towards stimulation and inhibition of the AR. The obtained results indicate that the method, single cell PSA secretion on membranes, is only useful for high-producing cell lines. The obtained results from low-producing cell lines are comparable to the negative control. This method fails to distinguish between PSA secretion and unspecific staining.

To overcome this problem, a microwell chip can be used. Using this chip, the secretion spots on the membrane can be correlated with the cells in the chip. To confirm if a spot is actually protein secretion, the corresponding well with the cell can be evaluated. The presence of a cell in the microwell can confirm the possibility of secretion. Otherwise, it can be regarded as unspecific staining or artefacts on the membranes. The microwell chip was tested using LNCaP cells and the results are quite promising in detecting and correlating the secretions with single cells.

Another advantage of using a microwell chip is that it shows the potential to identify the secretome from many cell lines. Different (stained) cell lines could be seeded simultaneously in the same chip and analysed for their protein secretion. This is time and cost-efficiently. In addition, using a microwell chip, the application multiplexing on membranes could be explored. The PVDF membranes can be coated with different coating antibodies, to simultaneously detect the secretion of different proteins. Another advantage of the microwell chip is that cells of interest can be punched out of the microwell chip and can be used for further research. This way the secretion level of a single cell can be correlated with other characteristics of the single cell, for example, their gene expression.

A limitation that needs to be addressed in this project, is the quantification method. Further optimization is recommended to improve the current quantification method, which is based on the fluorescent intensity of the spot. A more optimized method could take into account the circularity and fading of a spot. PSA secretion spots from LNCaP cells on membranes are clear round spots, which fade at the edges. However, artifacts are shown as small round spots with sharp edges, or as spots with an odd shape. Taking circularity and fading into account, could improve the quantification method to distinguish between spots and unspecific staining.

Another limitation that needs to be addressed is the lack of a standard curve. To make the PSA secretion data quantitative, a reliable calibration curve is needed. This experiment should be repeated with the previously described PSA concentrations. The exact quantitative data can then be compared with the literature and the results of the ELISA. The ELISA must also be repeated with the recommended dilution factors for supernatant of the cell lines. This will result in more reliable quantitative values. In addition, in a next ELISA experiment, both the PSA concentration of the supernatant of the cell lines as the PSA concentration of lysed cells can be explored. This way the difference between secreted PSA concentrations and cellular PSA concentrations can be determined.

This research fails to culture patient-derived organoids EMC-PCa-41. Due to the difficulties in growing the EMC-PCa-41 organoid cells, these cells could not be characterized and assessed for their responses to treatment. It is known that the success rate for obtaining and culturing patient-derived organoids from PCa patients is very low (Mout et al., 2021)(CHEAITO et al., 2022). The organoid cell line EMC-PCa-41 was kindly provided by Erasmus. More guidance from Erasmus in

culturing this organoid cell line would be beneficial. Culturing with some of the established PCa organoid cell lines such as MSK-PCa-1 and MSK-PCa2 can be utilized to develop preliminary models. Following this, culturing and characterization of EMC-PCa-41 can be performed to check for PSA and PSMA protein, secretion of PSA and the influence of anti-androgens such as Enzalutamide and other clinically relevant drugs such as Abiraterone and Docetaxel.

Another recommendation for future research is to explore other interesting secretome biomarkers in PCa. Such as the AR, prostate-specific cytokines and cathepsins K. In addition, the gene expression of different cell lines after stimulation and inhibition of the AR can be evaluated to provide a better understanding of the effect of treatment on these cell lines and determine possible correlation with the proteomic analysis. Together genotypic and proteomic analysis of single cells can help in identify prognostic biomarkers and develop an effective and personalized treatment for prostate cancer patients.

References

Abali, F., Baghi, N., Mout, L., Broekmaat, J. J., Tibbe, A. G. J., & Terstappen, L. W. M. M. (2021). Measurement of the Drug Sensitivity of Single Prostate Cancer Cells. *Cancers 2021, Vol. 13, Page 6083*, *13*(23), 6083. https://doi.org/10.3390/CANCERS13236083

Attardi, B. J., Burgenson, J., Hild, S. A., & Reel, J. R. (2004). Steroid hormonal regulation of growth, prostate specific antigen secretion, and transcription mediated by the mutated androgen receptor in CWR22Rv1 human prostate carcinoma cells. *Molecular and Cellular Endocrinology*, *222*(1–2), 121–132. https://doi.org/10.1016/J.MCE.2004.04.013

Bello, D., Webber, M. M., Kleinman, H. K., Wartinger, D. D., & Rhim, J. S. (1997). Androgen responsive adult human prostatic epithelial cell lines immortalized by human papillomavirus 18. *Carcinogenesis*, *18*(6), 1215–1223. https://doi.org/10.1093/CARCIN/18.6.1215

Bhamre, S., Whitin, J. C., & Cohen, H. J. (2003). Selenomethionine does not affect PSA secretion independent of its effect on LNCaP cell growth. *The Prostate*, *54*(4), 315–321. https://doi.org/10.1002/PROS.10184

Carm, K. T., Hoff, A. M., Bakken, A. C., Axcrona, U., Axcrona, K., Lothe, R. A., … Løvf, M. (2019). Interfocal heterogeneity challenges the clinical usefulness of molecular classification of primary prostate cancer. *Scientific Reports*, *9*(1). https://doi.org/10.1038/S41598-019-49964-7

Catalona, W. J. (2018). Prostate Cancer Screening. *The Medical Clinics of North America*, *102*(2), 199. https://doi.org/10.1016/J.MCNA.2017.11.001

Chandrasekar, T., Yang, J. C., Gao, A. C., & Evans, C. P. (2015). Mechanisms of resistance in castration-resistant prostate cancer (CRPC). *Translational Andrology and Urology*, *4*(3), 365. https://doi.org/10.3978/J.ISSN.2223-4683.2015.05.02

Chang, S. S. (2004). Overview of Prostate-Specific Membrane Antigen. *Reviews in Urology*, *6*(Suppl 10), S13. Retrieved from /pmc/articles/PMC1472940/

Chang, S. S., Reuter, V. E., Heston, W. D. W., & Gaudin, P. B. (2001). Comparison of anti-prostate-specific membrane antigen antibodies and other immunomarkers in metastatic prostate carcinoma. *Urology*, *57*(6), 1179–1183. https://doi.org/10.1016/S0090-4295(01)00983-9

CHEAITO, K., BAHMAD, H. F., HADADEH, O., MSHEIK, H., MONZER, A., BALLOUT, F., … ABOU-KHEIR, W. (2022). Establishment and characterization of prostate organoids from treatment-naïve patients with prostate cancer. *Oncology Letters*, *23*(1), 1–16. https://doi.org/10.3892/OL.2021.13124/HTML

Czaplicka, M., Niciński, K., Nowicka, A., Szymborski, T., Chmielewska, I., Trzcińska-Danielewicz, J., … Kamińska, A. (2020). Effect of Varying Expression of EpCAM on the Efficiency of CTCs Detection by SERS-Based Immunomagnetic Optofluidic Device. *Cancers*, *12*(11), 1–21. https://doi.org/10.3390/CANCERS12113315

Dathathri, E., Isebia, K. T., Abali, F., Lolkema, M. P., Martens, J. W. M., Terstappen, L. W. M. M., & Bansal, R. (2022). Liquid Biopsy Based Circulating Biomarkers in Metastatic Prostate Cancer. *Frontiers in Oncology*, *0*, 2236. https://doi.org/10.3389/FONC.2022.863472

Day, K. C., Hiles, G. L., Kozminsky, M., Dawsey, S. J., Paul, A., Broses, L. J., … Day, M. L. (2017). HER2 and EGFR overexpression support metastatic progression of prostate cancer to bone. *Cancer Research*, *77*(1), 74. https://doi.org/10.1158/0008-5472.CAN-16-1656

De Velasco, M. A., Kura, Y., Ando, N., Sako, N., Banno, E., Fujita, K., … Uemura, H. (2021). Context-Specific Efficacy of Apalutamide Therapy in Preclinical Models of Pten-Deficient Prostate Cancer. *Cancers*, *13*(16). https://doi.org/10.3390/CANCERS13163975

Deep, G., Oberlies, N. H., Kroll, D. J., & Agarwal, R. (2008). Isosilybin B causes androgen receptor degradation in human prostate carcinoma cells via PI3K-Akt-Mdm2-mediated pathway. *Oncogene 2008 27:28*, *27*(28), 3986–3998. https://doi.org/10.1038/onc.2008.45

Dent, S., Oyan, B., Honig, A., Mano, M., & Howell, S. (2013). HER2-targeted therapy in breast

cancer: a systematic review of neoadjuvant trials. *Cancer Treatment Reviews*, *39*(6), 622–631. https://doi.org/10.1016/J.CTRV.2013.01.002

Donato, M. T., Tolosa, L., & Gómez-Lechón, M. J. (2015). Culture and Functional Characterization of Human Hepatoma HepG2 Cells. *Methods in Molecular Biology (Clifton, N.J.)*, *1250*, 77–93. https://doi.org/10.1007/978-1-4939-2074-7_5

Donswijk, M. L., Van Leeuwen, P. J., Vegt, E., Cheung, Z., Heijmink, S. W. T. P. J., Van Der Poel, H. G., & Stokkel, M. P. M. (2020). Clinical impact of PSMA PET/CT in primary prostate cancer compared to conventional nodal and distant staging: a retrospective single center study. *BMC Cancer*, *20*(1). https://doi.org/10.1186/s12885-020-07192-7

Duffy, M. J. (2020). Biomarkers for prostate cancer: prostate-specific antigen and beyond. *Clinical Chemistry and Laboratory Medicine*, *58*(3), 326–339. https://doi.org/10.1515/CCLM-2019-0693

Girling, J. S., Whitaker, H. C., Mills, I. G., & Neal, D. E. (2007). Pathogenesis of prostate cancer and hormone refractory prostate cancer. *Indian Journal of Urology : IJU : Journal of the Urological Society of India*, *23*(1), 35. https://doi.org/10.4103/0970-1591.30265

Gorges, T. M., Riethdorf, S., von Ahsen, O., Nastaly, P., Röck, K., Boede, M., … Pantel, K. (2016). Heterogeneous PSMA expression on circulating tumor cells - a potential basis for stratification and monitoring of PSMA-directed therapies in prostate cancer. *Oncotarget*, *7*(23), 34930–34941. https://doi.org/10.18632/ONCOTARGET.9004

Harshman, L. C., Chen, Y. H., Liu, G., Carducci, M. A., Jarrard, D., Dreicer, R., … Sweeney, C. J. (2018). Seven-Month Prostate-Specific Antigen Is Prognostic in Metastatic Hormone-Sensitive Prostate Cancer Treated With Androgen Deprivation With or Without Docetaxel. *Journal of Clinical Oncology : Official Journal of the American Society of Clinical Oncology*, *36*(4), 376–382. https://doi.org/10.1200/JCO.2017.75.3921

Huggins, C. (1942). EFFECT OF ORCHIECTOMY AND IRRADIATION ON CANCER OF THE PROSTATE. *Annals of Surgery*, *115*(6), 1192. https://doi.org/10.1097/00000658-194206000-00030

IKNL. (2021). NKR Cijfers. Retrieved May 21, 2022, from https://iknl.nl/nkr-cijfers?fs%257Cepidemiologie_id=526&fs%257Ctumor_id=345&fs%257Cregio_id=550&fs%257Cperiode_id=564%252C565%252C566%252C567%252C568%252C569%252C570%252C571%252C572%252C573%252C574%252C575%252C576%252C577%252C578%252C579%252C580%252C581%252C582%252C583%252C584%252C585%252C586%252C587%252C588%252

Jemaa, A. Ben, Sallami, S., Céraline, J., & Oueslati, R. (2013). A novel regulation of PSMA and PSA expression by Q640X AR in 22Rv1 and LNCaP prostate cancer cells. *Cell Biology International*, *37*(5), 464–470. https://doi.org/10.1002/CBIN.10055

Keller, L., Werner, S., & Pantel, K. (2019). Biology and clinical relevance of EpCAM. *Cell Stress*, *3*(6), 165. https://doi.org/10.15698/CST2019.06.188

Kuske, A., Gorges, T. M., Tennstedt, P., Tiebel, A. K., Pompe, R., Preißer, F., … Pantel, K. (2016). Improved detection of circulating tumor cells in non-metastatic high-risk prostate cancer patients. *Scientific Reports*, *6*. https://doi.org/10.1038/SREP39736

Laidler, P., Dulińska, J., Lekka, M., & Lekki, J. (2005). Expression of prostate specific membrane antigen in androgen-independent prostate cancer cell line PC-3. *Archives of Biochemistry and Biophysics*, *435*(1), 1–14. https://doi.org/10.1016/J.ABB.2004.12.003

LI, S. G., & LI, L. (2013). Targeted therapy in HER2-positive breast cancer. *Biomedical Reports*, *1*(4), 499. https://doi.org/10.3892/BR.2013.95

Liao, Y., Wu, M., Jia, Y., Mou, R., & Li, X. (2022). EpCAM as a Novel Biomarker for Survivals in Prostate Cancer Patients. *Frontiers in Cell and Developmental Biology*, *0*, 869. https://doi.org/10.3389/FCELL.2022.843604

Malmberg, J., Tolmachev, V., & Orlova, A. (2011). Imaging agents for in vivo molecular profiling of disseminated prostate cancer: Cellular processing of [111In]-labeled CHX-A″DTPA-trastuzumab and anti-HER2 ABY-025 Affibody in prostate cancer cell lines. *Experimental*

and Therapeutic Medicine, *2*(3), 523. https://doi.org/10.3892/ETM.2011.217
Massoner, P., Thomm, T., Mack, B., Untergasser, G., Martowicz, A., Bobowski, K., … Puhr, M. (2014). EpCAM is overexpressed in local and metastatic prostate cancer, suppressed by chemotherapy and modulated by MET-associated miRNA-200c/205. *British Journal of Cancer*, *111*(5), 955–964. https://doi.org/10.1038/BJC.2014.366
Mathy, C. S., Mayr, T., Kürpig, S., Meisenheimer, M., Dolscheid-Pommerich, R. C., Stoffel-Wagner, B., … Bundschuh, R. A. (2021). Antihormone treatment differentially regulates PSA secretion, PSMA expression and 68Ga–PSMA uptake in LNCaP cells. *Journal of Cancer Research and Clinical Oncology*, *147*(6), 1733–1743. https://doi.org/10.1007/S00432-021-03583-W/FIGURES/5
Mitsiades, N., & Kaochar, S. (2021). Androgen receptor signaling inhibitors: post-chemotherapy, pre-chemotherapy and now in castration-sensitive prostate cancer. *Endocrine-Related Cancer*, *28*(8), T19–T38. https://doi.org/10.1530/ERC-21-0098
Mout, L., van Dessel, L. F., Kraan, J., de Jong, A. C., Neves, R. P. L., Erkens-Schulze, S., … Lolkema, M. P. (2021). Generating human prostate cancer organoids from leukapheresis enriched circulating tumour cells. *European Journal of Cancer*, *150*, 179–189. https://doi.org/10.1016/J.EJCA.2021.03.023
Narayanan, R. (2020). Therapeutic targeting of the androgen receptor (AR) and AR variants in prostate cancer. *Asian Journal of Urology*, *7*(3), 271–283. https://doi.org/10.1016/J.AJUR.2020.03.002
Ng, K., Smith, S., & Shamash, J. (2020). Metastatic Hormone-Sensitive Prostate Cancer (mHSPC): Advances and Treatment Strategies in the First-Line Setting. *Oncology and Therapy*, *8*(2), 209. https://doi.org/10.1007/S40487-020-00119-Z
Ni, J., Cozzi, P. J., Duan, W., Shigdar, S., Graham, P. H., John, K. H., & Li, Y. (2012a). Role of the EpCAM (CD326) in prostate cancer metastasis and progression. *Cancer and Metastasis Reviews*. https://doi.org/10.1007/s10555-012-9389-1
Ni, J., Cozzi, P. J., Duan, W., Shigdar, S., Graham, P. H., John, K. H., & Li, Y. (2012b). Role of the EpCAM (CD326) in prostate cancer metastasis and progression. *Cancer Metastasis Reviews*, *31*(3–4), 779–791. https://doi.org/10.1007/S10555-012-9389-1
Perlmutter, M. A., & Lepor, H. (2007). Androgen Deprivation Therapy in the Treatment of Advanced Prostate Cancer. *Reviews in Urology*, *9*(Suppl 1), S3. Retrieved from /pmc/articles/PMC1831539/
Qin, J., Liu, X., Laffin, B., Chen, X., Choy, G., Jeter, C. R., … Tang, D. G. (2012). Cell Stem Cell The PSA-/lo Prostate Cancer Cell Population Harbors Self-Renewing Long-Term Tumor-Propagating Cells that Resist Castration. https://doi.org/10.1016/j.stem.2012.03.009
Sasaki, T., Ishii, K., Iwamoto, Y., Kato, M., Miki, M., Kanda, H., … Sugimura, Y. (2016). Fibroblasts prolong serum prostate-specific antigen decline after androgen deprivation therapy in prostate cancer. *Laboratory Investigation; a Journal of Technical Methods and Pathology*, *96*(3), 338–349. https://doi.org/10.1038/LABINVEST.2015.136
Sharifi, N., Salmaninejad, A., Ferdosi, S., Bajestani, A. N., Khaleghiyan, M., Estiar, M. A., … Shakoori, A. (2016). HER2 gene amplification in patients with prostate cancer: Evaluating a CISH-based method. *Oncology Letters*, *12*(6), 4651. https://doi.org/10.3892/OL.2016.5235
Sheehan, B., Neeb, A., Buroni, L., Paschalis, A., Riisnaes, R., Gurel, B., … de Bono, J. (2022). Prostate-Specific Membrane Antigen Expression and Response to DNA Damaging Agents in Prostate Cancer. *Clinical Cancer Research*, OF1–OF12. https://doi.org/10.1158/1078-0432.ccr-21-4531
Siegel, R. L., Miller, K. D., & Jemal, A. (2020). Cancer statistics, 2020. *CA: A Cancer Journal for Clinicians*, *70*(1), 7–30. https://doi.org/10.3322/CAAC.21590
Staniszewska, M., Fragoso Costa, P., Eiber, M., Klose, J. M., Wosniack, J., Reis, H., … Iking, J. (2021). Enzalutamide Enhances PSMA Expression of PSMA-Low Prostate Cancer. *International Journal of Molecular Sciences*, *22*(14).

https://doi.org/10.3390/IJMS22147431
Strimbu, K., & Tavel, J. A. (2010). What are Biomarkers? *Current Opinion in HIV and AIDS*, *5*(6), 463. https://doi.org/10.1097/COH.0B013E32833ED177
Tai, S., Sun, Y., Squires, J. M., Zhang, H., Oh, W. K., Liang, C. Z., & Huang, J. (2011). PC3 is a cell line characteristic of prostatic small cell carcinoma. *Prostate*, *71*(15), 1668–1679. https://doi.org/10.1002/pros.21383
Tang, D. G. (2022). Understanding and targeting prostate cancer cell heterogeneity and plasticity. *Seminars in Cancer Biology*, *82*, 68–93. https://doi.org/10.1016/J.SEMCANCER.2021.11.001
Terada, N., Akamatsu, S., Kobayashi, T., Inoue, T., Ogawa, O., & Antonarakis, E. S. (2017). Prognostic and predictive biomarkers in prostate cancer: latest evidence and clinical implications. *Therapeutic Advances in Medical Oncology*, *9*(8), 565. https://doi.org/10.1177/1758834017719215
The American Cancer Society. (2020). Survival Rates for Prostate Cancer. Retrieved May 25, 2022, from https://www.cancer.org/cancer/prostate-cancer/detection-diagnosis-staging/survival-rates.html#references
Theil, G., Bialek, J., Weiß, C., Lindner, F., & Fornara, P. (2022). Strategies for Isolating and Propagating Circulating Tumor Cells in Men with Metastatic Prostate Cancer. *Diagnostics (Basel, Switzerland)*, *12*(2). https://doi.org/10.3390/DIAGNOSTICS12020497
Tikkinen, K. A. O., Dahm, P., Lytvyn, L., Heen, A. F., Vernooij, R. W. M., Siemieniuk, R. A. C., … Agoritsas, T. (2018). Prostate cancer screening with prostate-specific antigen (PSA) test: a clinical practice guideline. *BMJ*, *362*. https://doi.org/10.1136/BMJ.K3581
Tonry, C., Finn, S., Armstrong, J., & Pennington, S. R. (2020). Clinical proteomics for prostate cancer: understanding prostate cancer pathology and protein biomarkers for improved disease management. *Clinical Proteomics 2020 17:1*, *17*(1), 1–31. https://doi.org/10.1186/S12014-020-09305-7
Tse, B. W. C., Cowin, G. J., Soekmadji, C., Jovanovic, L., Vasireddy, R. S., Ling, M. T., … Russell, P. J. (2015). PSMA-targeting iron oxide magnetic nanoparticles enhance MRI of preclinical prostate cancer. *Nanomedicine*, *10*(3), 375–386. https://doi.org/10.2217/NNM.14.122/ASSET/IMAGES/LARGE/FIGURE6.JPEG
Tsechelidis, I., & Vrachimis, A. (2022). PSMA PET in Imaging Prostate Cancer. *Frontiers in Oncology*, *12*, 170. https://doi.org/10.3389/FONC.2022.831429/BIBTEX
Vellky, J. E., & Ricke, W. A. (2020). Development and prevalence of castration-resistant prostate cancer subtypes. *Neoplasia (New York, N.Y.)*, *22*(11), 566. https://doi.org/10.1016/J.NEO.2020.09.002
Wade, C. A., & Kyprianou, N. (2018). Profiling Prostate Cancer Therapeutic Resistance. *International Journal of Molecular Sciences*, *19*(3). https://doi.org/10.3390/IJMS19030904
Wenzel, M., Würnschimmel, C., Nocera, L., Collà Ruvolo, C., Tian, Z., Shariat, S. F., … Karakiewicz, P. I. (2021). Overall Survival After Systemic Treatment in High-volume Versus Low-volume Metastatic Hormone-sensitive Prostate Cancer: Systematic Review and Network Meta-analysis. *European Urology Focus*. https://doi.org/10.1016/J.EUF.2021.04.003
Xia, L., Wen, L., Meng, X., Zhou, N., Guo, X., Liu, T., … Yang, Z. (2021). Application Analysis of 124 I-PPMN for Enhanced Retention in Tumors of Prostate Cancer Xenograft Mice. *International Journal of Nanomedicine*, *16*, 7685–7695. https://doi.org/10.2147/IJN.S330237
Xu, Y., Zhao, H., & Hou, J. (2014). Correlation between overexpression of EpCAM in prostate tissues and genesis of androgen-dependent prostate cancer. *Tumour Biology : The Journal of the International Society for Oncodevelopmental Biology and Medicine*, *35*(7), 6695–6700. https://doi.org/10.1007/S13277-014-1892-2
Yamamoto, T., Gotoh, M., Koide, N., Funahashi, Y., Shimizu, S., & Takei, Y. (2020). Influence of human adipose stem cells on prostate cancer cell growth. *Nagoya Journal of Medical*

Science, *82*(2), 217–224. https://doi.org/10.18999/NAGJMS.82.2.217

Supplementary data

Calibration curve

The calibration curve is shown in Supplementary Figure 1. Low PSA concentrations resulted in dots with speckles (Supplementary Figure 2 and 3) and the highest PSA concentrations appeared saturated in the calibration curve (the two rightmost points in Supplementary Figure 1). This resulted in a low R-value (0.7066). Dismissing the two rightmost points, resulted in four points with a linear trendline, with a high R-value (0.9749)(trendline not shown). However, the quantitative data resulting from both trendlines in the calibration curve was not in line with the quantitative data of the ELISA and literature. Therefore, relative data will be used in the PSA secretion experiments. In future studies, it is recommended to repeat the experiment, to create a calibration curve, with the following PSA concentrations of 0 to 300 µg/mL in a serial dilution.

The area obtained from Image J was given in pixels. The formula to calculate the area in μm^2 is: Area (μm^2) = ((area (pixel)/16)*0.65)^2. In next experiments, the known size of a pixel should be filled in in the settings of the Image J software, as seen in: recommendation to quantification protocol in the Supplementary Data.

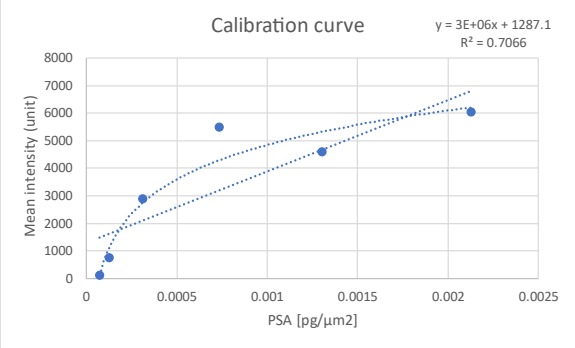

Supplementary Figure 1: Calibration curve PSA dilutions

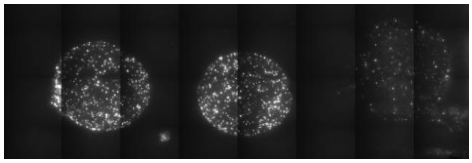

Supplementary Figure 2: PSA dilution spots with a PSA concentration of 2.3 µg/mL.

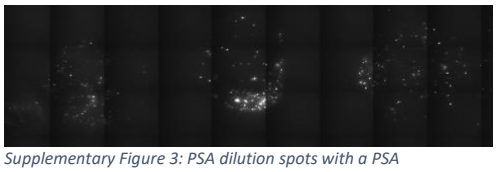

Supplementary Figure 3: PSA dilution spots with a PSA concentration of 0.6 µg/mL.

Overview characteristics datasets

Due to a change in microscopic fibre during the experiments, there is a change in exposure time and intensity threshold. These changes are presented in Supplementary Table 1.

Supplementary Table 1: Properties different dataset PSA secretion

Dataset	Cell line	Fiber type	Exposure time	Intensity threshold
04-02	RWPE-1, LNCaP, 22Rv1, PC-3, HEPG2	Old	50 ms	550
10-02	PWR-E1, RWPE-1, RWPE-2, LNCaP, 22Rv1, PC-3, HEPG2	Old	50 ms	550
18-02	PWR-E1, RWPE-1, RWPE-2, LNCaP, 22Rv1, PC-3, HEPG2	New	20 ms	5500
05-04	PWR-E1, RWPE-2, HEPG2, empty membrane	New	20 ms	5500

Quantification method

1. Create montage from individual images in image J:
    a. Drag the folder with individual images to the software Image J.
    b. The following pop-up appears (Supplementary Figure 4). Choose: 'Use virtual stack'.
    c. Go to: *Image → Stacks → Make montage*
    d. Save montage as tiff file: *File → Save as*

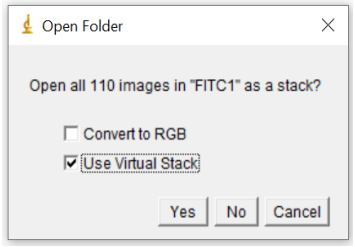

Supplementary Figure 4: Open Folder

2. Duplicate the montage and adjust it
    a. Go to: *Image → Duplicate*
    b. Adjust the brightness of the image, go to: *Image → Adjust → Brightness and contrast*
    c. Click on Set: the following pop-up appears (Supplementary Figure 5). Fill the following values in and press OK.
        i. Minimum displayed value: 0
        ii. Maximum displayed value: 1023
        iii. Unsigned 16-bit range: 10-bit
    d. Click on Apply in the 'Brightness and contrast' pop-up.

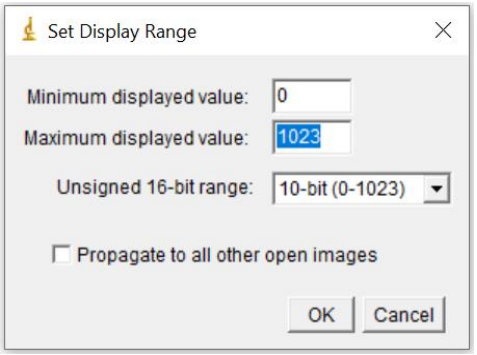

Supplementary Figure 5: Set display range

3. Set an intensity threshold

    a. Click on the duplicated 10-bit image

    b. Go to: *Image* → *Adjust* → *Threshold*

    c. The following pop-up appears (Supplementary Figure 6)

    d. Choose an intensity threshold value by dragging the bar or filling in exact numbers. In this case, a minimum intensity threshold of 550 is set.

    e. Press: Apply. A binary image is created.

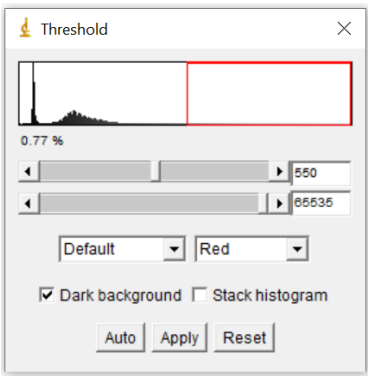

Supplementary Figure 6: Choose an intensity threshold

4. Set measurements

    a. Go to: *Analyze* → *Set Measurements*

    b. The following pop-up appears (Supplementary Figure 7). Choose the factors which you want to measure.

    c. Redirect to the original image (not the binary image).

    d. Press: OK.

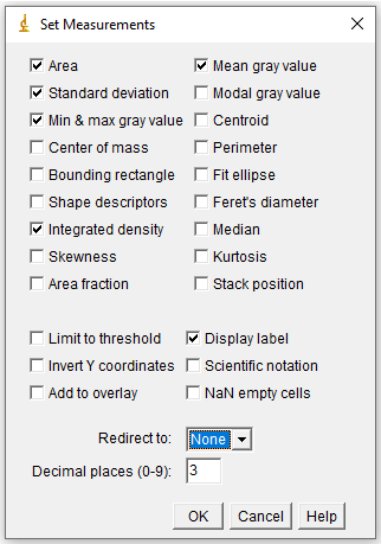

Supplementary Figure 7: Set Measurements

5. Analyse particles
    a. Go to: *Analyze* → *Analyze Particles*
    b. The following pop-up appears (Supplementary Figure 8). Choose the minimum/maximum pixel size.
        i. LNCaP cells: 4-infinity
        ii. Other cell lines: 0-infinity
    c. Circularity: 0-1
    d. Show: Outlines
    e. Choose: Display results, clear results, exclude on edges, include holes
    f. Press: OK. A pop-up with the results appears.

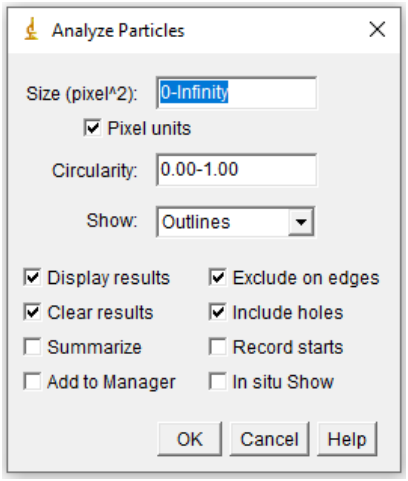

Supplementary Figure 8: Analyze Particles

6. Process data
    a. Copy the data to excel
    b. Measure the mean intensity of the belonging membrane with HEPG2 cells and subtract this mean intensity from all individual spot mean intensities.
    c. Multiply the individual mean intensities by the area. This result in a value which says something about the amount of PSA that is secreted.
    d. Calculate these values for the negative control: HEPG2. Calculate the mean value of the spots of HEPG2 cells. Take only values into account with a value higher than the mean value of the spots of HEPG2 cells. Plot these values.
    e. In case there exists a reliable calibration curve, use the formula from the linear trend-line:
        i. pg/μm^2 = (Mean intensity/a)-b
            1. Mean intensity of the spots is known.
            2. (*a* and *b* are obtained from the formula of the calibration curve).
        ii. Multiply the calculated 'pg/μm^2' by the size of the spot (in μm^2)

iii. This results in the amount of PSA in pg of one spot.

Recommendations protocol

- Set scale. Go to*: Analyze* → *Set scale.*
- It is known that when using an objective of 10x, 1 pixel equals 0.65 µm. Fill this in (Supplementary Figure 9).

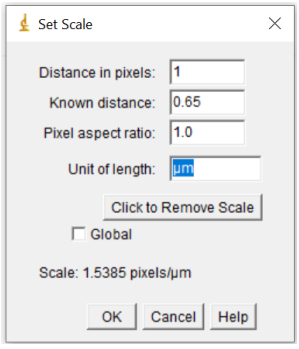

Supplementary Figure 9: Set scale.

Immunofluorescence staining on HEPG2 cells

In Supplementary Figure 10 the immunofluorescence images of HEPG2 cells are shown. However, no specific PSA and PSMA is observed.

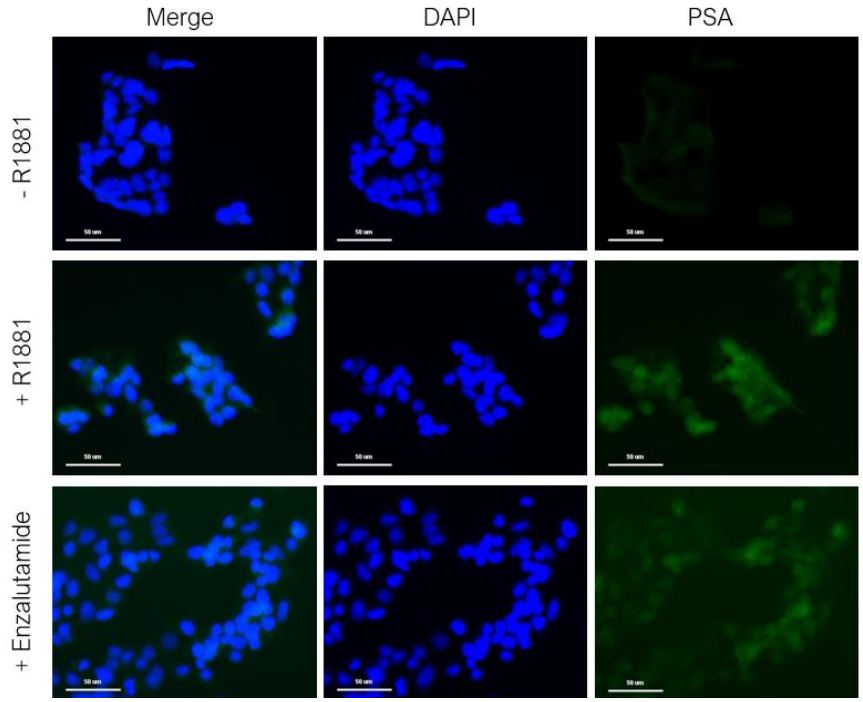

Supplementary Figure 10: Immunofluorescence detection of both PSA and PSMA expression in HEPG2 cells following androgen stimulation (R1881) or Enzalutamide treatment. Cell nuclei were counterstained with DAPI (blue). A,b,c) Untreated HEPG2 cells. d,e,f) Androgen stimulated (R1881) HEPG2 cells. F,h,i) Enzalutamide treated HEPG2 cells. Specific fluorescence signals for PSA (green) were not detected outside the nuclei. No signals for PSMA were detected in HEPG-2 cells (not shown). Scale bar: 50 µm

Intensity difference individual image

A membrane with spotted supernatant of LNCaP cells is shown in Supplementary Figure 11a. Vertical black lines in the spots are observed. From the pixels yellow line, the gray values are plotted and presented in Supplementary Figure 11b. A difference in gray value is observed in each individual image.

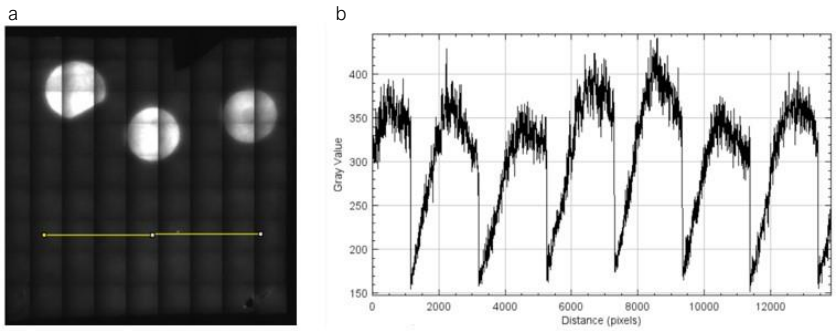

Supplementary Figure 11: Difference in intensity in each individual image

Negative control spots medium EMC-PCa-41

Dim spots of spotted medium of EMC-PCa-41 cells are shown in Supplementary Figure 12. The spots are indicated with red arrows.

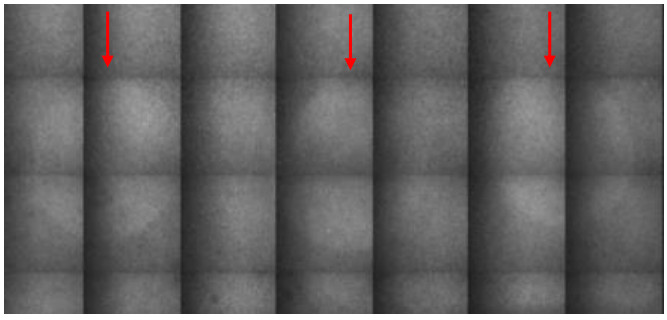

Supplementary Figure 12: Dim spots of medium EMC-PCa-41.

Threshold considerations

In Supplementary Figure 13 a membrane of 22Rv1 cells is shown in which a threshold of 550 is set. The red dots with a blue circle are taken into account as a PSA secretion spot with this threshold. However the white spots without a blue circle are not taken into account as PSA secretion with this threshold. Upon decreasing the intensity threshold, so that also these spots are taken into account, it turns out that also a lot of background signal is detected (Supplementary Figure 14). This is not favourable and reliable. Therefor is decided to keep the threshold of 550.

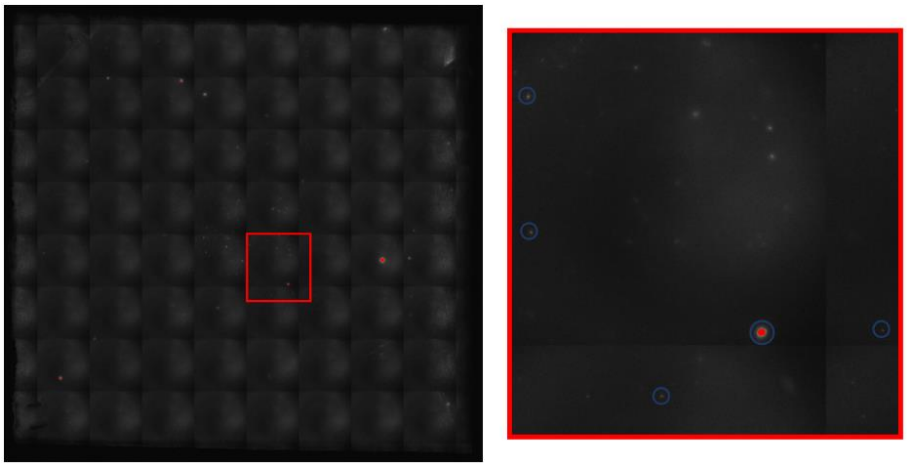

Supplementary Figure 13: Intensity threshold of 550 units on membrane of 22Rv1 cells. Red spots red dots with a blue circle are taken into account as PSA secretion spots. The white spots without a blue circle are not taken into account as PSA secretion.

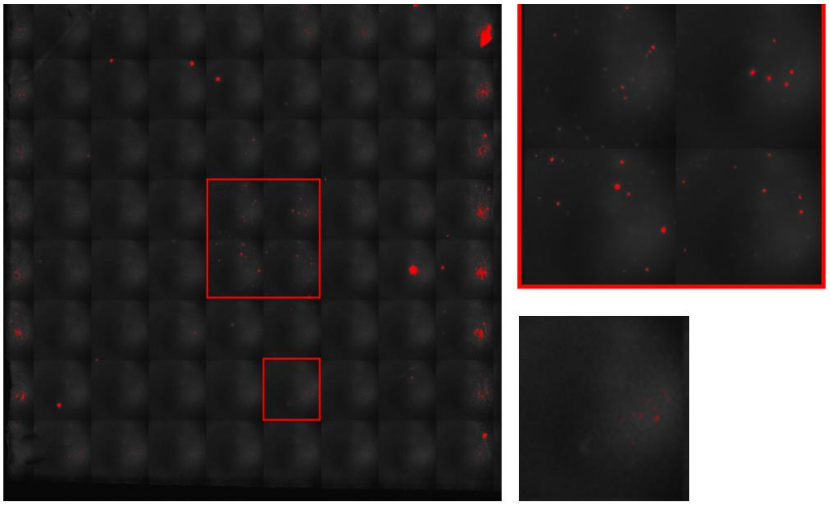

Supplementary Figure 14: Intensity threshold of 280 units on membrane of 22Rv1 cells. Red spots are taken into account as PSA secretion spots.

Graphs PSA secretion single cells

In Figure 36 an overview of PSA secretion of the different PCa cell lines is shown. In these Supplementary Figures 15-19, the PSA secretion graphs of the individual cell lines are shown.

For the cell lines: PWR-E1 and RWPE-2 applies N=1 (dataset 10-2), N=2 (dataset 18-02), N=3 (dataset 5-4). For the cell lines RWPE-1, 22Rv1 and PC-3 applies N=1 (dataset 4-2), N=2 (dataset 10-02) and N=3 (dataset 18-02).

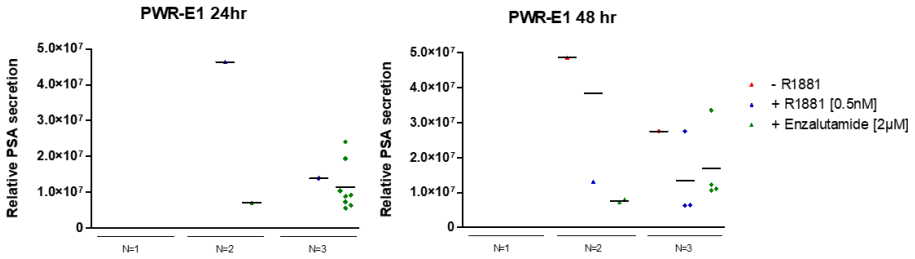

Supplementary Figure 15: Detected PSA secretion of single PWR-E1 cells after 24 and 48 hour under different conditions. The black line represents the mean. No clear trend was observed. Data was normalized to the HEPG2 cell line.

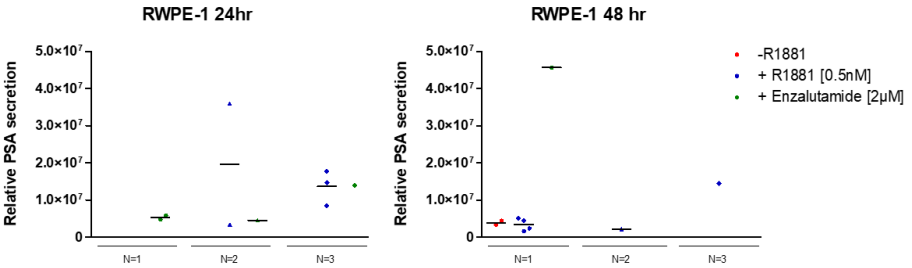

Supplementary Figure 16: Detected PSA secretion of single RWPE-1 cells after 24 and 48 hour under different conditions. The black line represents the mean. No clear trend was observed. Data was normalized to the HEPG2 cell line.

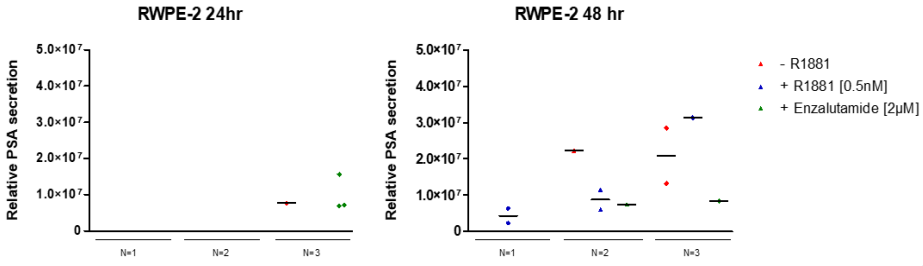

Supplementary Figure 17: Detected PSA secretion of single RWPE-2 cells after 24 and 48 hour under different conditions. The black line represents the mean. No clear trend was observed. Data was normalized to the HEPG2 cell line.

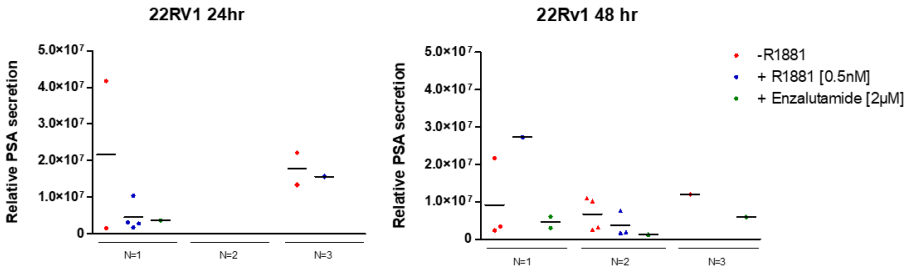

Supplementary Figure 18: Detected PSA secretion of single 22Rv1 cells after 24 and 48 hour under different conditions. The black line represents the mean. No clear trend was observed. Data was normalized to the HEPG2 cell line.

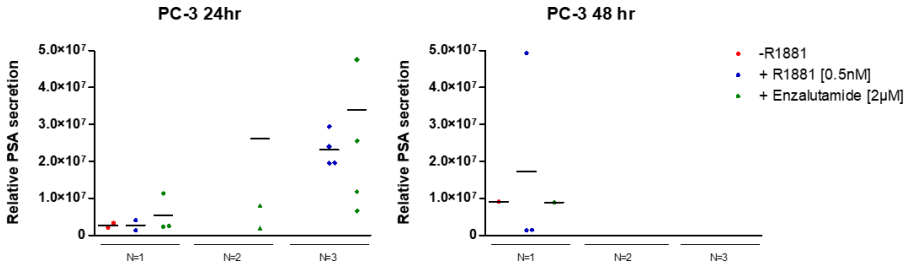

Supplementary Figure 19: Detected PSA secretion of single PC-3 cells after 24 and 48 hour under different conditions. The black line represents the mean. No clear trend was observed. Data was normalized to the HEPG2 cell line.